Geochemistry: Exploration, Environment, Analysis

Recent advances in the application of mineral chemistry to exploration for porphyry copper–gold–molybdenum deposits: detecting the geochemical fingerprints and footprints of hypogene mineralization and alteration

--Manuscript Draft--

Manuscript Number:	geochem2019-039R2
Article Type:	Research article
Full Title:	Recent advances in the application of mineral chemistry to exploration for porphyry copper–gold–molybdenum deposits: detecting the geochemical fingerprints and footprints of hypogene mineralization and alteration
Short Title:	Mineral chemistry applied to porphyry exploration
Corresponding Author:	David R Cooke, Ph.D. University of Tasmania Faculty of Science Engineering and Technology Hobart, Tas AUSTRALIA
Corresponding Author E-Mail:	d.cooke@utas.edu.au
Other Authors:	Paul Agnew
	Pete Hollings
	Michael Baker
	Zhaoshan Chang
	Jamie J. Wilkinson
	Ayesha Ahmed
	Noel C. White
	Lejun Zhang
	Jennifer Thompson
	J. Bruce Gemmell
	Huayong Chen
Abstract:	In the past decade, significant research efforts have been devoted to mineral chemistry studies to assist porphyry exploration. These activities can be divided into two major fields of research: (1) porphyry indicator minerals (PIMs), which are used to identify the presence of, or potential for, porphyry-style mineralization based on the chemistry of magmatic minerals such as zircon, plagioclase and apatite, or resistate hydrothermal minerals such as magnetite; and (2) porphyry vectoring and fertility tools (PVFTs), which use the chemical compositions of hydrothermal minerals such as epidote, chlorite and alunite to predict the likely direction and distance to mineralized centers, and the potential metal endowment of a mineral district. This new generation of exploration tools has been enabled by advances in and increased access to laser ablation-inductively coupled plasma mass spectrometry (LA-ICP-MS), short wave length infrared (SWIR), visible near-infrared (VNIR) and hyperspectral technologies. PIMs and PVFTs show considerable promise for exploration and are starting to be applied to the diversity of environments that host porphyry and epithermal deposits globally. Industry has consistently supported development of these tools, in the case of PVFTs encouraged by several successful blind tests where deposit centers have successfully been predicted from distal propylitic settings. Industry adoption is steadily increasing but is restrained by a lack of the necessary analytical equipment and expertise in commercial laboratories, and also by the on-going reliance on well-established geochemical exploration techniques (e.g., sediment, soil and rock-chip sampling) that have aided the discovery of near-surface resources over many decades,
Section/Category:	Exploration 17

Manuscript Classifications:	Base Metals; Exploration Geochemistry; Gold and PGEs
Additional Information:	
Question	**Response**
Are there any conflicting interests, financial or otherwise?	No
Samples used for data or illustrations in this article have been collected in a responsible manner	Confirmed
Response to Reviewers:	We have made the minor additional revisions requested by the editor. A revised version of the text is attached

Recent advances in the application of mineral chemistry to exploration for porphyry copper–gold–molybdenum deposits: detecting the geochemical fingerprints and footprints of hypogene mineralization and alteration

Cooke, David R.[1,2], Agnew, Paul[3], Hollings, Pete[4], Baker, Michael[1,2], Chang, Zhaoshan[5], Wilkinson, Jamie J.[6]], Ahmed, Ayesha[1,2], White, Noel C.[2,7], Zhang, Lejun[1,2], Thompson, Jennifer[1,2], Gemmell, J. Bruce[1,2], and Chen, Huayong[8]

1. ARC Research Hub for Transforming the Mining Value Chain, University of Tasmania, Private Bag 79. Hobart, Tasmania, 7001, Australia.
2. CODES, Centre for Ore Deposit and Earth Sciences, University of Tasmania, Private Bag 79, Hobart, Tasmania, 7001, Australia.
3. Rio Tinto Exploration, Research Avenue, Bundoora, Victoria, 3083, Australia.
4. Geology Department, Lakehead University, 955 Oliver Road, Thunder Bay, Ontario, P7B 5E1, Canada.
5. Colorado School of Mines, Golden, CO, 80401, USA.
6. LODE, Department of Earth Sciences, Natural History Museum, London SW7 5BD, UK.
7. Ore Deposit and Exploration Centre (ODEC), School of Resources and Environmental Engineering, Hefei University of Technology, Hefei 230009, Anhui, China.
8. Guangzhou Institute of Geochemistry, Chinese Academy of Sciences, 511 Kehua Street, Tianhe, PO Box 1131, Guangzhou, 510640, China.

ABSTRACT

In the past decade, significant research efforts have been devoted to mineral chemistry studies to assist porphyry exploration. These activities can be divided into two major fields of research: (1) porphyry indicator minerals (PIMs), which are used to identify the presence of, or potential for, porphyry-style mineralization based on the chemistry of magmatic minerals such as zircon, plagioclase and apatite, or resistate hydrothermal minerals such as magnetite; and (2) porphyry vectoring and fertility tools (PVFTs), which use the chemical compositions of hydrothermal minerals such as epidote, chlorite and alunite to predict the likely direction and distance to mineralized centers, and the potential metal endowment of a mineral district. This new generation of exploration tools has been enabled by advances in and increased access to laser ablation-inductively coupled plasma mass spectrometry (LA-ICP-MS), short wave length infrared (SWIR), visible near-infrared (VNIR) and hyperspectral technologies. PIMs and PVFTs show considerable promise for exploration and are starting to be applied to the diversity of environments that host porphyry and epithermal deposits globally. Industry has consistently supported development of these tools, in the case of PVFTs encouraged by several successful blind tests where deposit centers have successfully been predicted from distal propylitic settings. Industry adoption is steadily increasing but is restrained by a lack of the necessary analytical equipment and expertise in commercial laboratories, and also by the on-going reliance on well-established geochemical exploration techniques (e.g., sediment, soil and rock-chip sampling) that have aided the discovery of near-surface resources over many decades, but

are now proving less effective in the search for deeply buried mineral resources, and for those concealed under cover.

INTRODUCTION

The first half of the past decade saw a dramatic ramp up in global exploration expenditure, followed by an equally dramatic decline in expenditure in the latter half, accompanied by one of the harshest downturns in the mining sector in living memory. Over this time, discovery rates have simply not matched the record levels of expenditure (Fig. 1), and those discoveries being made were increasingly in areas of post mineral cover and at increasing depth (Schodde, 2017). Never has it been so important to have effective geochemical exploration tools, but the challenge in developing and applying them is significant. Geochemical exploration is undoubtedly most effective when searching for outcropping or near-surface mineralization. As exploration increasingly focusses on deeper targets and moves inexorably into areas of post-mineralization cover, the role of geochemistry in exploration programs is changing.

New geochemical techniques and technologies are needed urgently or the role of geochemistry in making new discoveries will continue to decline. Porphyry-related copper, gold and molybdenum deposits, and their related epithermal gold, silver ± copper ore zones, continue to be attractive exploration targets for major mining companies, with a notable increase in discoveries under cover in the past two decades. Advances in geophysical exploration techniques, and/or deep drilling, have contributed to several spectacular examples of recent porphyry and high sulfidation epithermal deposit discoveries (e.g., Ridgeway, Cadia East, Hugo Dummett, Resolution, Pebble East, Cukaru Peki; Holliday and Cooke, 2007).

Geochemical exploration techniques have mostly failed to have the same impact as geophysical exploration methods during the past two decades, due partly to the challenges associated with modification or destruction of hypogene geochemical anomalies by supergene phenomena, and also because of difficulties detecting anomalies beneath syn- and post-mineralization cover. Cost-effective geochemical exploration programs need to maximize the information that can be obtained in early exploration stages. This is particularly true in exploration settings on the edge of cover or when targeting deeper porphyry systems. In these increasingly common scenarios, conventional geochemical signals are weak, alteration is distal, erratic and difficult to separate from background sources with very similar mineral assemblages. Cost-effective, low-density geochemical techniques that rapidly focus exploration activity into proximal settings can therefore be of real value to industry. The UNCOVER Australia initiative has identified the development of appropriate geochemical tools for exploration under cover as a national priority (Rowe, 2017).

Recently, significant efforts have been expended in mineral chemistry research aimed at aiding porphyry exploration. The recognition of fertile belts of igneous intrusions and prospective areas of hydrothermal alteration can now be assisted through the use of porphyry indicator minerals (PIMs) such as zircon, plagioclase, apatite, magnetite and tourmaline (Dupuis and Beaudoin, 2011; Dilles et al., 2015; Shen et al., 2015; Williamson et al., 2016; Bouzari et al., 2016) – such minerals can help to identify the geochemical ‘fingerprint’ of a porphyry deposit and discriminate it from other deposit styles and background rocks. At the district scale, far-field detection of concealed mineralized centers in porphyry districts has been enabled through the application of porphyry vectoring and fertility tools (PVFTs), which involves detection of low-level geochemical anomalies preserved in hydrothermal alteration minerals such

as epidote, chlorite or alunite (Chang et al., 2011; Cooke et al., 2014a, 2015, 2017; Wilkinson et al., 2015, 2017; Baker et al., 2017; Xiao et al., 2018). This new generation of geochemical exploration tools have been created due to advances in laser ablation-inductively coupled plasma mass spectrometry (LA-ICP-MS) and hyperspectral analytical techniques. Some PVFTs have the potential to significantly extend the dimensions of the detectable geochemical 'footprint' of porphyry deposits outwards by several kilometers into the very weakly-altered rocks that surround these large hydrothermal systems.

This article reviews new advances in PIM and PVFT research in the context of the porphyry exploration model, highlighting how these new tools can add value to exploration campaigns for porphyry deposits. Key aspects of porphyry deposits are also reviewed to provide context for the discussion of PIMs and PVFTs.

PORPHYRY DEPOSITS

Porphyry deposits are the world's largest repositories of copper and molybdenum and are major sources of gold and silver. Peripheral mineralization styles (e.g., skarns, carbonate replacement deposits and epithermal veins) can be enriched in zinc, lead and silver. Some porphyry deposits are significantly endowed with tin and/or tungsten. Porphyry deposits are one of the key exploration targets for major mining companies. Their characteristics are well-documented (Sillitoe, 1989, 2000, 2010; Seedorff et al., 2005; Cooke et al., 2014b) and exploration models are well-developed (Lowell and Guilbert, 1970; Gustafson and Hunt, 1975; Holliday and Cooke, 2007). The following sections review key aspects of porphyry deposits and their environments of formation that are pertinent to a discussion of PIMs and PVFTs.

Geodynamic settings

Most porphyry deposits have a spatial and temporal association with active plate margins (Sillitoe, 2010, 2012). The continental arc settings of South and North America have been particularly productive for the formation of giant porphyry Cu-Mo deposits since the Cretaceous (Cooke et al., 2005). Tertiary and Quaternary oceanic arc settings in the SW Pacific, Central America and the Caribbean and parts of the Tethyan belt have produced significant Cu-Au porphyry deposits. Porphyry deposits have also formed in collisional settings such as China and Papua New Guinea (Hou et al., 2009, 2011; Richards, 2009, 2011a; Haschke et al., 2010; Pirajno and Zhou, 2015). Back-arc environments have also been favorable for alkalic porphyry deposits (Hollings et al., 2011; Wolfe and Cooke, 2011).

Porphyry deposits typically form in environments that promote rapid uplift and exhumation (Cooke et al., 2005; Hollings et al., 2005). The deposits therefore have a low preservation potential in the ancient rock record (Wilkinson and Kesler, 2006; Kesler and Wilkinson, 2008; Yanites and Kesler, 2015), with most of the known porphyry deposits being Cretaceous, Tertiary or Quaternary in age. Older examples are known – for example, Paleozoic porphyry deposits are exposed in the Central Asian orogenic belt (Shen et al., 2015), eastern Australia (Harris et al., 2013) and Canada (Shelton, 1983), Mesozoic porphyry deposits are well-exposed in western Canada (Bissig and Cooke, 2014) and Paleoproterozoic examples are preserved in Sweden (Sillitoe, 2012). These older porphyry deposits generally formed in oceanic arc settings that were subsequently amalgamated to continental margins, with a transition of geodynamic settings from those promoting uplift and exhumation to those promoting burial being essential for their preservation.

Several countries and continents apparently lack porphyry deposits, despite being sites of modern or ancient subduction. Notable examples in young arc-related settings include New Zealand and Japan. The continent of Africa and subcontinent of India are underendowed with porphyry deposits – it remains an open question as to whether this is due to preservation issues, if these terrains were unfavorable for porphyry ore formation, or that they remain comparatively underexplored. Porphyry-style mineralization has been reported from the Antarctic Peninsula (Rowley et al., 1975; Hawkes and Littlefair, 1981), but the United Nations' Antarctic-Environmental Protocol prevents modern exploration of this potentially fertile terrain.

Intrusive complexes

Porphyry deposits take their name from shallow-crustal porphyritic intrusive complexes that are spatially, temporally and genetically related to porphyry-style alteration and mineralization. A large range of intrusive compositions have produced porphyry mineralization, with individual deposits associated with intermediate (diorite, quartz diorite) to felsic (monzonite, granodiorite, granite) compositions (Kesler et al., 1975; Seedorff et al., 2005; Audetat and Simon, 2012). Tonalites and syenites are also known to be associated with porphyry ores. Generally, Cu porphyries are associated with monzonites, granites and syenites, Au porphyries with diorites, Mo-porphyries with monzonites, granites and trondhjemites, and Sn-W porphyries with rhyolites and rhyodacites (Seedorff et al., 2005). Although a diverse spectrum of magmatic compositions has produced mineralization, we highlight a few key common characteristics that impact on porphyry exploration.

Porphyry deposits are typically associated with calc-alkaline to alkalic magmas that have intermediate to felsic compositions (Lang et al., 1995; Seedorff et al., 2005). The ultimate source of the shallow level intrusions is thought to be mafic arc magmas formed from low degrees of partial melting and the melting of magmatic sulfides in the lower crust (Hou et al., 2011; Audétat and Simon, 2012). Oxidized magmas are essential for effective magmatic transport of Cu, Au and Mo together with sulfur from the metasomatised mantle to the upper crust (Richards, 2015). The magmas are sulfur-bearing I-type, magnetite-series intrusions. Sulfur is transported primarily as SO_2 in the melt, preventing sequestration of chalcophile elements into immiscible sulfide droplets and thereby promoting co-transport with Cu, Au and Mo. The oxidized state of the magmas is reflected in the presence of primary magnetite as phenocrysts and/or groundmass phases. If the intrusive complex exsolved hydrothermal fluids, a domain of magnetite-bearing quartz veins and potassic alteration assemblages may form in and around the intrusive complex, particularly if it has an intermediate composition (Holliday and Cooke, 2007).

The intrusive complexes that produce porphyry deposits generate enormous volumes of magmatic-hydrothermal fluids. This requires extreme water contents in the melts (Richards, 2011b; Loucks, 2014). These hydrous melts can be recognized in the field by the presence of hornblende as a phenocryst phase. Stabilization of hornblende before plagioclase during the magmatic crystallization sequence can potentially produce adakite-like geochemical signatures, which may aid in greenfields exploration (Loucks, 2014). The simple recognition of hornblende as a phenocryst phase in intrusive complexes can be a favorable sign for the prospectivity of a suite of magmatic rocks for porphyry mineralization. Loucks (2014) and Richards (2011b) have suggested whole rock Sr/Y and V/Sc values can be used as proxies for high water contents in a magmatic system and consequently their potential to form porphyry systems. For example, Loucks (2012) showed that more than 80 porphyry Cu deposits worldwide may be genetically related to felsic intrusions with $Sr/Y > 35$.

Alteration assemblages

Porphyry-related alteration models are amongst the most utilized and robust in geosciences and have facilitated exploration and discovery for over half a century. Figure 2 highlights key alteration domains associated with mineralized porphyry complexes (Lowell and Guilbert, 1970; Gustafson and Hunt, 1975; Sillitoe, 2000, 2010; Seedorff et al., 2005; Holliday and Cooke, 2007). These models have proven highly effective for exploration vectoring into proximal setting and this can only be enhanced as the growing volume of high-resolution hyperspectral mineralogy expands our understanding of the true complexity of alteration assemblages as well as their vectoring and fertility potential.

Potassic core

There is typically a central domain of potassic alteration that develops in and around the mineralizing stock. The alteration is characterized by orthoclase, biotite, magnetite, quartz and anhydrite, spatially associated with quartz veins that contain chalcopyrite, bornite, gold and/or molybdenite. This domain is typically the host to high-grade mineralization and is the principal target in porphyry exploration. It may be overprinted by younger clay- and/or muscovite-rich alteration assemblages that in some cases add significant mineralization and in others may dilute or destroy grade.

Green rock environment

The potassic core is surrounded laterally by rocks that have undergone propylitic alteration, which can be divided into three sub-zones (Fig. 2). The inner propylitic subzone is rarely recognized, but is defined by the presence of actinolite, together with epidote, chlorite, calcite, albite ± hematite ± pyrite. This passes laterally outwards to the epidote subzone, which lacks actinolite, and then to the outer chlorite subzone, which lacks both actinolite and epidote. These subzones essentially map the actinolite and epidote isograds (Fig. 2) and represent decreasing fluid temperatures away from the intrusive complex (Cooke et al., 2014a). Magnetite and pyrite may be present as alteration minerals in both the actinolite and epidote subzones, but are best developed close to the intrusive complex, defining magnetite and pyrite alteration halos that can be detected using magnetic and IP surveys, respectively. Pyrite typically has a broader lateral dispersion than magnetite, so that porphyry deposits can have central magnetic highs surrounded by magnetic lows and variable chargeability anomalies, depending on the sulfide abundances, level of erosion and degree of overprinting by late-stage alteration assemblages. If reactive rocks such as limestones, dolomites, basalts, or ultramafic or silica-undersaturated volcanic rocks are present, then calc-silicate (skarn) alteration assemblages may form around the intrusive complex. Garnet, pyroxene and wollastonite are diagnostic alteration minerals, with retrograde epidote, amphibole, magnetite – hematite, chlorite, calcite, quartz and sulfides common as overprinting phases (Meinert et al., 2005).

Lithocaps

Lithocaps may form between the mineralizing intrusive complex and the paleosurface (Fig. 2). Lithocaps are large, stratabound domains of silicic, advanced argillic and argillic alteration assemblages that can exceed dimensions of 10 x 10 km laterally and may be more than 1 km thick (Sillitoe, 1995; Chang et al., 2011; Cooke et al., 2017). Lithocaps typically have structural roots, with advanced argillic assemblages transitioning downwards from quartz – alunite – pyrite to quartz – dickite – pyrophyllite – pyrite and then into phyllic-altered roots (i.e., quartz – muscovite – pyrite; Sillitoe, 1999). Lithocaps provide significant challenges for explorers because they have very broad, difficult to detect lateral alteration zonation patterns defined by clay minerals (Chang et al., 2011; Cooke et al., 2017).

ENABLING TECHNOLOGIES

Mineral chemistry has been investigated as a potential tool to aid porphyry exploration for several decades (e.g., Ballantyne, 1981), but conventional analytical techniques such as the electron microprobe (EPMA) and wet chemical methods have a number of limitations such as high detection limits of EPMA and the need to obtain large volumes of clean monomineralic fractions for wet chemistry, that historically restricted the suite of trace elements that could be used to characterize mineral compositions, limiting the development of such tools. At the same time, clay mineral identification was proving challenging for porphyry explorers as it required access to time-consuming laboratory-based techniques such as X-ray diffraction. Development and widespread uptake of three key enabling technologies provided the basis for the development of PIMs and PVFTs in the first two decades of the twenty-first century.

LA-ICP-MS

The development of laser ablation-inductively coupled plasma mass spectrometry (LA-ICP-MS) in the late 1990s provided a robust and rapid alternative for mineral chemistry analyses. There are several distinct advantages of the LA-ICP-MS method over EMPA, including the ability to analyze many elements simultaneously, and detection limits that are several orders of magnitude lower than achievable using EMPA. Data processing and interpretation of LA-ICP-MS results is significantly more challenging than for EMPA, with rigorous quality assurance and quality control measures required to ensure that high quality and consistent geochemical data are generated by laser ablation laboratories. Recent advances in automation of LA-ICP-MS analyses, and new software for data processing and interpretation developed by CODES Analytical Laboratories (LADR, https://norsci.com/?p=software) have significantly increased throughput and decreased the amount of time required for robust data interpretation.

SEM-based techniques

This decade has seen the first use of SEM-based automated mineralogy technology such as MLA™ and QEMSEM™ for exploration purposes, and such techniques can be a boon for indicator mineral analyses. Layton-Matthews et al (2014) demonstrated the value of automated mineralogy on fine fraction till heavy mineral concentrates for detection of glacial indicator mineral trains associated with VHMS-style deposits. Whilst industry use of automated mineralogy for exploration remains focused on a few early adopters, there is a significant opportunity in the coming decade to greatly enhance the utility and cost effectiveness of PIMs. Going forward, the optimal workflow for PIMS and PVFTs analyses is likely to involve initial SEM-based automated mineralogical identification of appropriate minerals, followed by geochemical analyses by LA-ICP-MS.

Short wave and near-infrared spectrometry

In the late 1990s, field-portable short-wave length infrared devices became widely available, facilitating real-time clay mineral identification in the field. Portable SWIR detectors such as the PIMA-SP® and PNIRS®, and VNIR detectors such as the TerraSpec® Halo have proven to be essential aids for mapping and exploring porphyry and high sulfidation deposits and the lithocaps that can host or obscure them. The past decade has also seen the emergence and rapid uptake of hyperspectral core scanning technology (e.g., Hylogger®, Corescan® and TerraCore®; Jackson et al., 2018). These scanning technologies have delivered a step-change in the capacity for explorers and miners to robustly recognize and semi-quantify the abundances of a wide range of spectrally active minerals at resolutions as low as 500 μm. While hyperspectral technologies are particularly relevant to porphyry and epithermal exploration, they have

also proven to have applications for many commodities across the mining value chain, from exploration to feasibility assessments, to mineral processing, geotechnical assessments and waste characterization (Jackson et al., 2018). By combining high resolution reflectance spectroscopy, visual imagery and 3D laser profiling, it is now possible to automatically log spectrally active mineralogy, rock and mineral textures and geotechnical features down-hole in a rapid, robust and repeatable fashion (e.g., Harraden et al., 2019; Fig. 3).

PORPHYRY INDICATOR MINERALS (PIMS)

Indicator minerals preserve signals of their source environment and can be sampled from transported clastic media during geochemical exploration, provided that the indicator mineral is resistant to weathering (McClenaghan, 2005). Some of the minerals that form in porphyry copper systems can be considered as porphyry indicator minerals (PIMs) – these are magmatic or hydrothermal minerals with distinctive compositions that discriminate them from the same minerals sampled from other environments, such as barren wall rocks or other mineralization styles (Fig. 4). Kimberlitic indicator minerals have been used intensively in the diamonds exploration industry since the early 1980s and have been instrumental in the discovery of many of the world's diamond deposits (Gurney et al., 1993). PIMs have similar potential to assist in the discovery of porphyry Cu systems, particularly those that are either poorly exposed or eroded and concealed under post-mineralization cover.

There are two main categories of PIMs – those that are indicative of potentially fertile magmatic suites, such as zircon, plagioclase and apatite (Shen et al., 2015; Williamson et al., 2016; Bouzari et al., 2016; Loader et al., 2017), and resistate hydrothermal minerals that may be preserved in eroded materials (e.g., stream sediments, soil, till; Fig. 4), such as tourmaline, garnet, epidote, pyrite, magnetite, gold and rutile (Kelley et al., 2011; Eppinger et al., 2013). Some PIMs can be used to discriminate magmatic and hydrothermal environments (e.g., magnetite, apatite, titanite; Dupuis and Beaudoin, 2011; Dare et al., 2014; Celis et al., 2014; Pisiak et al., 2017). We briefly review the characteristics of zircon, plagioclase, apatite and magnetite below.

Zircon

The intermediate to felsic intrusive complexes that produce porphyry Cu deposits typically contain zircon as a magmatic accessory phase. Zircon is a key mineral for analysis in porphyry environments, both because it provides the most robust high temperature geochronometer available for magmatic rocks (von Quadt et al. 2011; Chiaradia et al., 2013; Buret et al., 2016, 2017), and for the profound insights into magma petrogenesis that can be gained from analyses of its isotopic and trace element compositions. Key information gained from trace elements in zircons include: (i) magmatic oxidation states from Ce and Eu anomalies (Ballard et al., 2002; Hoskin and Schaltegger, 2003; Burnham and Berry, 2012; Dilles et al., 2015; Shen et al., 2015), (ii) the temperature of zircon crystallization from Ti content (Ferry and Watson, 2007; Watson and Harrison, 2005), and (iii) evolving magma composition from variations in Zr/Hf, U, Th and REE patterns (Claiborne et al., 2006; Kemp et al., 2007).

Positive Ce anomalies and negative Eu anomalies in zircon are indicative of oxidized magmas (Ballard et al., 2002; Dilles et al., 2015). In their study of a range of large and small (in terms of Cu endowment) Paleozoic porphyry Cu-Au deposits of the Central Asian Orogenic Belt, Shen et al. (2015) documented a relationship between the oxidation state of the magmas, as recorded by the Ce^{4+}/Ce^{3+} values for zircons, and the Cu endowment of the deposit. The intermediate to large deposits all have Ce^{4+}/Ce^{3+} values above

120, whereas the small deposits and a comparative dataset of barren Paleozoic granitoids of the Lachlan Fold belt of Australia (Belousova et al., 2006) have much lower Ce^{4+}/Ce^{3+} values (Fig. 5). However, the Ce and Eu anomalies in zircon can be strongly dependent on melt REE contents, which are usually poorly constrained, and can also be controlled by the crystallization of titanite and other REE-bearing phases. Consequently, these REE anomalies are not regarded as especially robust proxies for melt oxidation state (Loader et al., 2017). On-going research needs to test whether zircon trace element chemistry can aid porphyry exploration globally, or if it is useful only in specific terranes, and whether false positives are a potential issue. It is likely that using combination of zircon trace element chemistry and whole rock geochemistry will be a focus of companies seeking to identify fertile porphyry-bearing belts in underexplored terrains over the next decade.

Plagioclase

Magmatic plagioclase is abundant as both a phenocryst and groundmass phase in porphyry-related intrusive complexes (Seedorff et al., 2005). Hydrothermal albite is a common alteration product in parts of porphyry systems. Calcic plagioclase occurs more rarely as a hydrothermal phase, particularly in skarns and calc-sodic alteration assemblages (Dilles and Einaudi, 1992). Magmatic plagioclase is commonly altered by hydrothermal processes, and may be replaced by orthoclase (e.g., potassic zone), albite, epidote and/or calcite (e.g., propylitic zone), muscovite/illite (phyllic zone), alunite, pyrophyllite, dickite and/or kaolinite (advanced argillic zone). It is therefore uncommon to find magmatic plagioclase compositions well-preserved in the core of porphyry Cu environments. The reactive and commonly altered nature of plagioclase, coupled with its low density, limits its potential as a resistate mineral in exploration.

Magmatic plagioclase has potential to be used as a PIM. Williamson et al. (2016) noted that igneous plagioclase from the world's largest porphyry Cu-Mo district in terms of contained Cu metal, Rio Blanco – Los Bronces (Chile), had excess Al contents when compared to typical arc magmas from the Caribbean that are unrelated to porphyry Cu deposits (Fig. 6). The excess Al is interpreted to be related to high magmatic water contents that were produced by injection of hydrous fluids or fluid-rich melts into the parental magma chamber (Williamson et al., 2016). Elevated H_2O contents in porphyry ore-forming magmas are an essential prerequisite for porphyry mineralization (Loucks, 2014). Along with whole rock geochemistry and zircon trace element geochemistry, plagioclase compositions may therefore contribute to prospectivity assessments in greenfields targeting exercises. There are, however, two important caveats to this approach: (1) the plagioclase must have pristine magmatic compositions – it cannot be weakly altered or weathered, and (2) the analytical method must be high quality, as the plagioclase compositional variations between fertile and barren intrusions are small (Fig. 6) and analytical errors could create issues with detection.

Apatite

Apatite can form in diverse geological environments, including magmatic and hydrothermal settings (Belousova et al., 2002; Hughes and Rakovan, 2015; Webster and Picoli, 2015). Mao et al. (2016) showed that discriminant projection analyses can effectively distinguish apatite from magmatic and a variety of hydrothermal environments, including porphyry, skarn, epithermal, Kiruna, IOCG and orogenic deposits. Furthermore, they were able to define distinctive compositions of apatites from various subtypes of porphyry deposits (i.e., Cu-Mo-Au, Mo and alkalic Cu-Au) and skarn deposits (W vs. Au-Co, Cu and Pb-Zn skarns). A combination of apatite mineral chemistry and apatite cathodoluminescence has been used to discriminate magmatic apatite and several varieties of hydrothermal apatite from different alteration

zones in selected porphyry deposits of British Columbia (Bouzari et al., 2016; Fig. 7), and also at Oyu Tolgoi, Mongolia, and Resolution, USA (Loader, 2017) and Chuquicamata, Chile (Brugge et al., 2017). These studies highlight that apatite has considerable potential as a PIM, and that it warrants more detailed investigation. Alkalic igneous rocks tend to be P-enriched (Crawford et al., 2007), and so apatite may have particular relevance as a PIM for alkalic porphyry deposits.

Magnetite

Magnetite has been considered a prospective indicator mineral for many years due to its resistive nature and ease of separation. Cross (2000) showed that major element ratios (Al//Ti vs V/Ti) could effectively discriminate magmatic and hydrothermal magnetites from porphyry and skarn deposits, and that the hydrothermal environments of magnetite alteration (porphyry vs skarn) could also be discriminated. Dupuis and Beaudoin (2011) took this further, arguing that major element chemistry (e.g., plots of Ca + Al + Mn vs Ti + V) can effectively discriminate magnetite from a diversity of ore deposit types. Using Reko Diq (Pakistan) as an example, Dupuis and Beaudoin (2011) highlighted that individual magnetite compositions may plot in several fields, but the average compositions plot in the relevant field for the deposit type of interest. Hu et al. (2015) showed that re-equilibration of magnetite from a single iron skarn deposit in China had produced magnetite compositions that plotted across several of the discrimination fields defined by Dupuis and Beaudoin (2011), highlighting potential challenges with this approach. Dare et al. (2014), Nadoll et al. (2015) and Pisiak et al. (2017) acquired major and trace element analyses of magnetite from a variety of igneous, porphyry and skarn environments. They used element ratios and statistical data exploration to demonstrate how magnetite compositions can effectively discriminate magnetite of diverse origins (e.g., Fig. 8). Sievwright (2018) extended these findings, illustrating how discriminant projection analysis of magnetite LA-ICP-MS data can effectively discriminate different populations of hydrothermal magnetite from porphyry deposits. Collectively, these studies inspire confidence that magnetite has considerable potential as a PIM.

For magmatic magnetite, LA-ICP-MS analyses can be advantageous for their potential to provide the average composition of the Fe-oxide precursor prior to exsolution as a function of varying P-T-fO_2 conditions (Dare et al., 2012). But there are two potential issues with regards LA-ICP-MS analyses of magmatic magnetite: (1) magnetite typically undergoes oxy-exsolution, and (2) it is prone to diffusional resetting by post-crystallization hydrothermal fluids (Sievwright, 2018). These issues require that care must be taken in analysis and data interpretation – the choice of analytical method (e.g., spot size) and appropriate and rigorous data processing quality assurance and quality control procedures are essential for the acquisition of high-quality representative LA-ICP-MS data from primary magnetite. For example, if exsolution lamellae are ablated together with magnetite, they may adversely contaminate the analysis. Some of these analytical challenges may have contributed to the inconsistent results obtained by previous workers when attempting to discriminate different varieties of magnetite (e.g., Hu et al., 2015).

PORPHYRY VECTORING AND FERTILITY TOOLS (PVFTS)

Since 2004, a series of AMIRA International research projects (P765, 765A, 1060, 1153, 1202) have been conducted at CODES (University of Tasmania) and collaborating organizations. These industry collaborative projects have been robustly supported by up to 21 industry sponsors, several of them over a period of more than 15 years, demonstrating the mineral industry's sustained interest in this research. The

research program has developed new geochemical and geological methods to detect, vector towards, and discriminate between porphyry and epithermal deposits from different environments. Analysis of subtle, low-level hypogene geochemical signals preserved in hydrothermal alteration minerals can potentially provide explorers with both fertility (how large? – i.e., is there potential for large, giant, or supergiant deposits?; terminology from Singer, 1995) and vectoring information (how far, and in what direction?), allowing the presence, location and relative metal endowment of porphyry and/or epithermal copper, gold and molybdenum deposits to be assessed during the early stages of exploration) with remarkably low-density sampling and very low cost relative to most other available search technologies (e.g., soil, stream sediment and rock chip sampling). These projects have delivered new porphyry vectoring and fertility exploration tools and have demonstrated their efficacy with several successful "blind tests" where deposit centers have successfully been predicted from distal propylitic settings (e.g., Cooke et al., in press).

PVFTs potentially have particular relevance to exploration on the edge of cover, and when drilling under post-mineralization cover, as well as in areas where outcrop is limited (e.g., heavily vegetated tropical settings). Vectoring assessments require in-situ sampling, as the location of the deposit is predicted using spatial variations in mineral chemistry that occur across the district. Consequently, PVFTs cannot be sampled from transported media. Research to date has focused on key alteration minerals in green rock environments (e.g., epidote and chlorite; Cooke et al., 2014a, 2015, in press; Wilkinson et al., 2015, 2017, in press; Baker et al., 2017, in press; Xiao et al., 2018; Pacey et al., in press; Fig. 2). Rio Tinto Exploration has routinely analyzed high volumes of chlorite and epidote from global porphyry Cu exploration programs since 2012 and remains committed to demonstrating the importance of this technology (Agnew, 2015).

Epidote

Epidote is a common alteration mineral in the propylitic halo to porphyry deposits, particularly those hosted in volcanic or plutonic rocks (Sillitoe, 2010). The relatively oxidizing conditions typical of porphyry copper environments tend to favor the formation of Fe^{3+}-bearing epidote over Al^{3+}-bearing clinozoisite, the Al^{3+}-rich end-member of the epidote-clinozoisite solid solution (Cooke et al., 2014a). In addition to Ca, Fe, Al, and Si, epidote group minerals can contain high concentrations of LREE and pathfinder elements such as As, Sb, Pb, V and Mn (Cooke et al., 2014a), making it particularly useful as a PVFT.

Cooke et al. (2014a) defined the green rock environment of porphyry systems as the background propylitic alteration domains that surround the porphyritic intrusive complexes and that underlie the lithocap. The geochemical dispersion of pathfinder elements from the potassic zone of porphyry deposits into the green rock environment creates geochemical zonation patterns of proximal Cu-Mo-Au surrounded by distal Zn-Pb-Mn-V-As-Sb that have been used for decades in porphyry exploration (e.g., Emmons, 1927; Halley et al., 2015). But conventional whole rock analyses in distal propylitic settings (i.e., outside of the pyrite halo; Fig. 2) commonly fail to detect geochemical anomalism at distances greater than 1 – 2 km from the porphyry centers due to dilution of pathfinder element concentrations by relict primary minerals (Cooke et al., 2014a). In these distal settings, epidote and chlorite LA-ICP-MS analyses have been shown to extend the detectable geochemical footprint of porphyry deposits by several kilometers relative to conventional rock chip sampling (Cooke et al., 2014a, in press; Wilkinson et al., 2015, in press; Baker et al., in press; Pacey et al., in press). Epidote also has the potential to be used as a PIM in exploration (e.g., epidote in

till samples – Kelley et al., 2011). It can potentially provide information regarding the presence of proximal or distal porphyry-style propylitic alteration that can then be followed up with PVFTs-style exploration once the bedrock alteration source is identified.

For green rocks, PVFTs sampling is generally guided by the field identification of epidote, which is visually distinctive due to its pistachio-green color. Epidote has wide distributions, both as replacement of other Ca-bearing minerals (e.g., plagioclase, hornblende), and as vein fill. Epidote veins can define an outer stockwork around the central quartz-rich stockwork and mapping of epidote vein and replacement intensity can be used to vector towards porphyry centers (Garwin, 2002; Cooke et al., 2014a). Epidote-bearing rock chips commonly contain chlorite, and so both minerals can be analyzed together during PVFT analyses. SWIR analyses can be obtained using a portable short-wave infrared detector during field sampling to help confirm the presence of epidote and/or chlorite in rock chip samples.

Epidote and/or chlorite-bearing samples are prepared for laser ablation analyses as one-inch diameter polished mounts. Epidote and chlorite grains from each laser mount are selected for analyses using reflected light microscopy. In-situ samples are analyzed rather than mineral separates as this allows the paragenetic context and modes of occurrence of the minerals of interest to be constrained during petrography, enhancing the metadata available for interpretation of the significance of the data (e.g., vein vs replacement; replacement of plagioclase, hornblende, K-feldspar, groundmass, etc.).

In a study of the porphyry Cu-Au deposits of the Baguio district, Philippines, Cooke et al. (2014a) showed how the trace element chemistry of epidote can vary with respect to proximity to porphyry mineralized centers, with distal pathfinder elements such as As, Sb and Pb enriched in epidote up to several kilometers away from the porphyry center. Furthermore, they demonstrated that the pathfinder elements were enriched in epidote around large, well-endowed (fertile) porphyry centers and were low in epidote from small porphyry deposits and/or sub-economic prospects. These results imply that epidote LA-ICP-MS analyses have potential both for vectoring and fertility assessments in green rock environments around porphyry deposits. Similar patterns of trace element enrichment and depletion in epidote have been detected around the El Teniente and Collahuasi porphyry Cu-Mo deposits, Chile (Wilkinson et al. 2017; in press; Baker et al., in press), the E48 porphyry Cu-Au deposit, Australia (Pacey et al., in press) and the Resolution porphyry Cu-Mo deposit, Arizona (Cooke et al., in press). LA-ICP-MS analyses can also be used to discriminate between hydrothermal (porphyry-related) and metamorphic epidote. Baker et al. (2017) showed that Sr/As and Pb/U ratios effectively discriminate metamorphic epidotes of Central Chile from porphyry-related epidotes in the same region, and from the Baguio dataset of Cooke et al. (2014a). The metamorphic epidotes are characterized by very low pathfinder element concentrations (particularly Sb, also As).

As an illustration of the potential application of epidote trace element chemistry to porphyry exploration, Figure 9 shows variations in the As content of epidote determined as part of a blind test of the Taldy Bulak porphyry Cu-Au deposit, Kyrgyzstan. Using a broad- spaced sample distribution (approximately one rock chip every 300 – 500 m), LA-ICP-MS analyses of epidote from the rock chip samples defined a domain characterized by low As in epidote that is broadly coincident with the > 600 ppm Cu in soils anomaly detected by Gold Fields Ltd. during their conventional geochemical exploration campaign. Low As in epidote has been recognized in several porphyry systems as a characteristic feature of epidote that grows together with pyrite in environments proximal to porphyry deposits (i.e., inside the pyrite halo – Cooke et

al., 2014a; in press; Fig 2). Any coprecipitating pyrite can scavenge the chalcophile elements preferentially resulting in epidote with relatively low metal contents, but once pyrite deposition has depleted H_2S from the fluid at the limits of the pyrite halo, any remaining metals are forced into silicate phases such as epidote (As, Sb, Pb) or chlorite (Cu, Zn), producing pathfinder metal-rich silicate alteration minerals distal to the porphyry center (Cooke et al., 2014a; in press). Consequently, for Taldy Bulak, the low As in epidote domain is interpreted to highlight the likely location of the sulfide-bearing alteration zones, which should be centered on the mineralized intrusive complex, consistent with the interpretation of the Cu in soils anomaly and the > 0.5 ppm Au in drill core intercepts (Fig. 9).

Chlorite

In their study of variations in chlorite compositions around the Batu Hijau porphyry Cu-Au deposit, Indonesia, Wilkinson et al. (2015) demonstrated that chlorite effectively provides vectors to the mineralized center of the deposit within 2.5 km and potentially up to 5 km. Chlorite has proven to be an effective vectoring tool because trace element substitution into the chlorite crystal lattice is strongly controlled by temperature and probably also by pH (Wilkinson et al., 2015), with elements such as Ti, Mg and V enriched in high temperature chlorite, and other elements such as Sr, Li, Co and Ni enriched in chlorite that forms at lower temperatures and/or higher pH. Element ratios (e.g., Ti/Sr; Mg/Sr, V/Ni) enhance the spatial variations and have been used to develop 'proximitor' equations (Wilkinson et al., 2015; Baker et al, in press) that can provide vectoring parameters that vary with distance from the deposit center by over four orders of magnitude. Wilkinson et al. (2017, in press) showed similar results for chlorite analyses from El Teniente, Chile. But in that case, the giant porphyry system produced a correspondingly much larger footprint, with the Ti/Li proximitor able to detect the presence of mineralization up to 5 km from the deposit center. Wilkinson et al. (2015) noted that the trace element contents of chlorite also show potential as a tool for fertility assessments in porphyry exploration.

The combination of epidote and chlorite LA-ICP-MS analyses of samples from green rock environments can help to effectively target porphyry deposits. Figure 9 shows that high Ti/Sr values for chlorite from the Taldy Bulak blind test, Kyrgyzstan, overlap with the As low defined from epidote analyses. The high values for Ti/Sr in chlorite are inferred to have shifted slightly northwards of the low As in epidote anomaly because the trace element compositions of the two minerals varied in response to different processes. The As concentrations in epidote are interpreted to be strongly influenced by the coprecipitating mineral phases, with low As concentrations typical of porphyry-related epidote that co-precipitates with pyrite (Cooke et al., 2014a). High temperatures are interpreted to favor high Ti/Sr values for chlorite, because Ti substitutes into chlorite at high temperatures, and Sr at low temperatures (Wilkinson et al., 2015). Consequently, high Ti/Sr in chlorite provide indications of proximity to the heat source, whereas low As in epidote provides indications of proximity to the sulfide zone. Both the As in epidote and Ti/Sr chlorite anomalies broadly coincide with the 600 ppm Cu in soils anomaly, providing a bulls eye target. A similar response was detected at El Teniente, Chile (Wilkinson et al., 2017; in press) and at Resolution, Arizona (Cooke et al., in press). This technology opens up low-cost exploration opportunities on the edge of post-mineral cover or for deep, uneroded porphyry systems including those which may be associated with lithocaps.

Alunite

Lithocaps are large stratabound alteration domains dominated by silicic and advanced argillic alteration assemblages (Sillitoe, 1995, Cooke et al., 2017; Fig. 2)). In the lithocap environment, explorers have been challenged by the huge volumes of intensely altered rocks because alteration zonation patterns are difficult to map due in part to the huge scale of the alteration domains, and the challenges associated with accurate field identification of fine-grained clay minerals. The advent of portable SWIR analyzers has transformed exploration in lithocaps, facilitating the mapping of spatial distributions of key alteration minerals such as alunite, pyrophyllite, dickite, illite and kaolinite, which has considerably aided vectoring to porphyry and high sulfidation mineralized centers.

Chang et al. (2011) undertook a systematic study of the Lepanto lithocap, Philippines, which hosts the Lepanto high sulfidation epithermal Cu-Au-Ag deposit and overlies the Far Southeast Cu-Au porphyry deposit. They showed that alunite is a key alteration mineral for exploration in this environment. Alunite has a temperature-dependent solid solution behavior between Na- (high temperature) and K- (low-temperature) end-members (Stoffregen and Cygan, 1990). Chang et al. (2011) showed that the Na and K contents of alunite control the 1480 nm absorption peak position of alunite detected by SWIR techniques. High temperature natroalunite (Na-alunite) has a peak position around 1496 nm, whereas K-alunite has peak positions around 1478. By systematically obtaining SWIR data across the Mankayan lithocap, Chang et al. (2011) demonstrated that higher wavelength values were detected above and near the Far South East porphyry (Fig. 10a), which is inferred to be the heat and fluid source for the Mankayan lithocap.

Chang et al. (2011) also demonstrated systematic variations in the trace element chemistry of alunite with respect to distance from the Far South East porphyry. Trace elements such as Sr and La are enriched in alunite close to the porphyry, and Pb (which substitutes for K in the alunite crystal structure) is enriched in distal settings. These mineralogical variations were detected by LA-ICP-MS and microprobe analyses and could be used to aid exploration in lithocaps.

A key advanced argillic alteration assemblage in lithocaps is defined by quartz and alunite. Chang et al. (2011) were able to demonstrate that the same geochemical anomalies detected by LA-ICP-MS analyses of alunite from the Mankayan lithocap could be detected using whole rock geochemistry, if rock chip samples were first screened using a combination of SWIR analysis and whole rock geochemistry. In order to detect the alunite trace element chemistry signature from whole rock data, SWIR analyses are used to first confirm that the altered rock contains alunite. Trace element screening of samples with <0.1% Cu and <0.1 ppm Au then eliminates any complications created by late-stage overprinting epithermal mineralization on the early-formed quartz-alunite alteration. After screening out non-alunite-bearing and strongly mineralized samples, Chang et al. (2011) demonstrated systematic spatial variations in trace element ratios from whole rock data, specifically 1000000 * Pb/(Na+K), Sr/Pb and 100 * La/Pb (Fig. 10b and c). These ratios varied with respect to proximity to the Far Southeast porphyry deposit, most likely due to temperature-controlled alunite trace element substitutions. The spatial patterns defined by these whole rock geochemical vectoring ratios mimic the variations detected by SWIR analyses of alunite (Fig. 10a). This combination of techniques has provided explorers with new field-based exploration tools that have been underpinned by knowledge gained from LA-ICP-MS and SWIR data and which are now used routinely in lithocap exploration.

CONCLUSIONS

As the world transitions towards widespread use of renewable energy, there is an increasing demand for copper that needs to be met at least in part by new discoveries of porphyry deposits. But the past decade was not outstanding for new porphyry discoveries, and going forward, industry geoscientists, researchers and service providers must embrace new and emerging technologies if geochemistry is to maintain a critical role in the discovery of new porphyry Cu resources under cover or in previously unrecognized greenfield terrains.

Recent technological advances have enabled low-level detection of trace element compositions of primary and alteration minerals via LA-ICP-MS, and rapid, automated clay mineral identification via hyperspectral techniques. These enabling technologies permitted researchers to demonstrate that some magmatic and hydrothermal minerals in porphyry environments have the potential to be either PIMs (e.g., zircon) or PVFTs (e.g., chlorite, alunite). There are also some minerals (e.g., epidote, apatite and magnetite) that can potentially be used both as a PIM and a PVFT, provided that in the case of PVFTs assessments, they are sampled directly from bedrock. The combination of mineral chemistry and hyperspectral analyses have the potential to aid in exploration for porphyry and epithermal deposits over the next decade, supplementing insights gained from conventional geochemical and geophysical techniques. LA-ICP-MS analyses of alteration minerals in green rock environments (epidote, chlorite) can potentially expand the detectable geochemical footprint of porphyry deposits for kilometers beyond what can be detected by whole rock geochemistry, significantly increasing the search radius for geochemical detection and potentially aiding exploration under cover by providing an additional method for vectoring from drilling into propylitic alteration. If the application of PIMs and/or PVFTs can impact favorably on a major porphyry or epithermal discovery in the next few years, then this would validate the methods and accelerate uptake of these innovative new geochemical exploration techniques.

ACKNOWLEDGEMENTS

We thank all of our research colleagues, sponsors and students (past and present) who have collaborated on AMIRA projects P765, P765A, P1060, P1153 and P1202. We thank Andrew Wurst, formerly of Gold Fields, for providing the Taldy Bulak blind site test to AMIRA project P765A. We also thank AMIRA coordinators Adele Seymon and Alan Goode for their tireless support of our work. Georges Beaudoin, John Barr, Charles Beaudry, Richard Preece, Nick Joyce and Christopher R Beckett-Brown are thanked for their critical comments that have helped to substantially improve this manuscript. The TMVC is an Australian Research Council (ARC)-funded Industrial Transformation Research Hub, and CODES is the Centre for Ore Deposit and Earth Sciences at the University of Tasmania. The ARC's support of our research is gratefully acknowledged. LODE is generously sponsored by Anglo American, Quantum Pacific Exploration and Rio Tinto. The support of the Natural History Museum and the Department of Earth Science and Engineering at Imperial College London are gratefully acknowledged.

REFERENCES

Agnew, P., 2015, What industry wants from research: Society of Economic Geologists, World Class Ore Deposits – Discovery to Recovery, Conference Proceedings, Hobart, Tasmania, 2 p.

Audétat, A., and A. Simon, 2012, Magmatic controls on porphyry copper genesis: Society of Economic Geologists, Special Publication 16, 553–572.

Baker, M., D.R. Cooke, P. Hollings and J. Piquer, 2017, Identification of hydrothermal alteration related to mineralisation using epidote mineral chemistry, in Mineral Resources to Discover: Society of Geology Applied to Ore Deposits, 14th Biennial Conference Proceedings, Quebec, v. 3, 1069–1071.

Baker, M.J., J.J. Wilkinson, C.C. Wilkinson, D.R. Cooke, and T.J. Ireland, in press, Epidote trace element chemistry as an exploration tool: a case study from the Collahuasi district, northern Chile: Economic Geology, in press.

Ballantyne, G.H., 1981, Chemical and mineralogical variations in propylitic zones surrounding porphyry copper deposits: Ph.D. thesis, University of Utah, 208 p.

Ballard, J.R., J.M. Palin, and I.H. Campbell, 2002, Relative oxidation states of magmas inferred from Ce(IV)/Ce(III) in zircon: Application to porphyry copper deposits of northern Chile: Contributions to Mineralogy and Petrology, v. 144, p. 347–364.

Belousova, E.A., Griffin, W.L., O'Reilly, S.Y., and Fisher, N.I., 2002, Apatite as an indicator mineral for mineral exploration: Trace-element compositions and their relationship to host rock type: Journal of Geochemical Exploration, v. 76, p. 45–69.

Belousova, E.A., W.L. Griffin, and S.Y. O'Reilly, 2006, Zircon crystal morphology, trace element signatures and Hf isotope composition as a tool for petrogenetic modelling: Examples from Eastern Australian granitoids: Journal of Petrology, 47, 329–353.

Bissig, T., and D.R. Cooke, 2014, Introduction to the special issue devoted to alkalic porphyry Cu-Au and epithermal Au deposits: Economic Geology, 109, 819–825.

Bouzari et al., 2016, Hydrothermal alteration revealed by apatite luminescence and chemistry: A potential indicator mineral for exploring covered porphyry copper deposits: Economic Geology, 111, 1397–1410.

Buret, Y., A.V. Quadt,, C. Heinrich, D. Selby, M. Wälle, and I. Peytcheva, 2016, From a long-lived upper-crustal magma chamber to rapid porphyry copper emplacement: Reading the geochemistry of zircon crystals at Bajo de la Alumbrera (NW Argentina): Earth and Planetary Science Letters, 450, 120 – 131.

Brugge, E., J.J. Wilkinson, and A. Miles, 2017, Habit and chemistry of apatite from Chuquicamata, Chile, in Mineral Resources to Discover: Society of Geology Applied to Ore Deposits, 14th Biennial Conference Proceedings, Quebec, 287–290.

Buret, Y., J.F. Wotzlaw, S. Roozen, M. Guillong, A.V. Quadt, and C. Heinrich, 2017, Zircon petrochronological evidence for a plutonic-volcanic connection in porphyry copper deposits: Geology, 45, doi: 10.1130/G38994.1.

Burnham, A.D., and A.J. Berry, 2012, An experimental study of trace element partitioning between zircon and melt as a function of oxygen fugacity: Geochimica et Cosmochimica Acta, 95, 196–212.

Celis, M.A., F. Bouzari, T. Bissig, C.J.R. Hart, and T. Ferbey, 2014, Petrographic characteristics of porphyry indicator minerals from alkalic porphyry copper-gold deposits in south-central British Columbia (NTS 092, 093): Geoscience BC, Summary of Activities 2013, 2014-1, 53–62.

Chang Z, J.W. Hedenquist, N.C. White, D.R. Cooke, M. Roach, C.L. Deyell, J. Garcia, J.B. Gemmell, S. McKnight, and A.L.Cuison, 2011, Exploration tools for linked porphyry and epithermal deposits: Example from the Mankayan intrusion-centered Cu-Au district, Luzon, Philippines: Economic Geology, 106, 1365–1398.

Chiaradia, M., U. Schaltegger, R. Spikings, J.F. Wotzlaw, and M. Ovtcharova, 2013, How accurately can we date the duration of magmatic-hydrothermal events in porphyry systems?—An invited paper: Economic Geology, 108, 565-584.

Claiborne, L.L., C.F. Miller, B.A. Walker, J.L. Wooden, F.K. Mazdab and F. Bea, 2006, Tracking magmatic processes through Zr/Hf ratios in rocks and Hf and Ti zoning in zircons: An example from the Spirit Mountain batholith, Nevada: Mineralogical Magazine, 70, 517-543.

Cooke, D.R., P. Hollings, and J. Walshe, 2005, Giant porphyry deposits – Characteristics, distribution and tectonic controls: Economic Geology 100: 801–818.

Cooke D.R., M. Baker, P. Hollings G. Sweet, Z. Chang, L. Danyushevsky, S. Gilbert, T. Zhou, N.C. White, J.B. Gemmell, and S. Inglis, 2014a, New advances in detecting systems – epidote mineral chemistry as a tool for vectoring and fertility assessments: Society of Economic Geologists, Special Publication 18, 127–152.

Cooke D.R., P. Hollings, J.J. Wilkinson, and R.M. Tosdal 2014b, Geochemistry of porphyry deposits, in: Holland H.D. and Turekian K.K. (eds.) Treatise on Geochemistry, Second Edition, v. 13, Oxford, Elsevier, p. 357–381.

Cooke, D.R., J.J. Wilkinson, M. Baker, P. Agnew, C.C. Wilkinson, H. Martin, Z. Chang, H. Chen, J.B. Gemmell, S. Inglis, L. Danyushevsky, S. Gilbert, and P. Hollings, 2015, Using mineral chemistry to detect the location of concealed porphyry deposits – an example from Resolution, Arizona: 27th International Association of Geochemistry Symposium – conference proceedings, USA, 20-24th April, p. 1–6.

Cooke, D.R., J.J. Wilkinson, M. Baker, P. Agnew, J. Phillips, Z. Chang, H. Chen, C.C. Wilkinson, S. Inglis, P. Hollings, J.B. Gemmell, N.C. White, L. Danyushevsky, and H. Martin, in press, Using mineral chemistry to aid exploration – a case study from the Resolution porphyry Cu-Mo deposit, Arizona: Economic Geology, in press.

Cooke D.R., N.C. White, L. Zhang, Z. Chang, and H. Chen, 2017, Lithocaps – characteristics, origins and significance for porphyry and epithermal exploration, in Mineral Resources to Discover: Society of Geology Applied to Ore Deposits, 14th Biennial Conference Proceedings, Quebec, 1, p. 219-294.

Crawford A.J., S. Meffre, R.J. Squire, L.M. Barron, and T.J. Falloon, 2007, Middle and Late Ordovician magmatic evolution of the Macquarie Arc, Lachlan Orogen, New South Wales: Australian Journal of Earth Sciences, 54, p. 181 – 214.

Cross, A.J., 2000, An investigation of the minor and trace element chemistry of hydrothermal porphyry and skarn-related magnetite: Ph.D. thesis, University of Canberra, 171 p.

Dare, S.A., S.-J. Barnes, G. Beaudoin, 2012, Variation in trace element content of magnetite crystallized from a fractionating sulfide liquid, Sudbury, Canada: implications for provenance discrimination: Geochimica Cosmochimica Acta, 88, 27–50

Dare, S.A., S.-J. Barnes, G. Beaudoin, J. Méric, E. Boutroy, and C. Potvin-Doucet, 2014, Trace elements in magnetite as petrogenetic indicators: Mineralium Deposita, 49, 785–796.

Dilles J.H., and M.T., Einaudi, 1992, Wall-rock alteration and hydrothermal flow paths about the Ann-Mason porphyry copper deposit, Nevada—a 6-km vertical reconstruction: Economic Geology, 87, 1963−2001.

Dilles, J.H., A.J.R. Kent, J.L. Wooden, R.M. Tosdal, A. Koleszar, R.G. Lee, and L.P. Farmer, 2015, Zircon compositional evidence for sulfur-degassing from ore-forming arc magmas: Economic Geology, 110, 241–251.

Dupuis, C., and G. Beaudoin, 2011, Discriminant diagrams for iron oxide trace element fingerprinting of mineral deposit types: Mineralium Deposita, 46, 319–335.

Emmons, W.H., 1927, Relations of the disseminated copper ores in porphyry to igneous intrusives: American Institute of Mining Metallurgists and Engineers Transactions, 75, 797-815.

Eppinger, R.G., D.L. Fey, S.A. Giles,, E. Grunsky, K.D. Kelley, B.J. Minsley, L. Munk, and S.M. Smith, 2013, Summary of exploration geochemical and mineralogical studies at the giant Pebble porphyry Cu-Au-Mo deposit, Alaska: Implications for exploration: Economic Geology, 108, 495–527.

Ferry, J.M., and E.B. Watson, 2007, New thermodynamic models and revised calibrations for the Ti-in-zircon and Zr-in-rutile thermometers: Contributions to Mineralogy and Petrology, 154, 429–437.

Garwin, S., 2002, The geologic setting of intrusion-related hydrothermal systems near the Batu Hijau porphyry copper-gold deposit, Sumbawa, Indonesia: Society of Economic Geologists Special Publication 9, p. 333–366.

Gurney, J.J., H. Helmstaedt, and R.O. Moore, 1993, A review of the use and application of mantle mineral geochemistry in diamond exploration: Pure & Applied Chemistry, 65, 2423-2442.

Gustafson, L.B., and J.P. Hunt, 1975, The porphyry copper deposit at El Salvador, Chile: Economic Geology, 70, 857–912.

Halley, S., J.H. Dilles, and R.M. Tosdal, 2015: Footprints: hydrothermal alteration and geochemical dispersion around porphyry copper deposits: SEG Newsletter, 100, 1, 12-17.

Harraden C.L., M.J. Cracknell, J. Lett, R.F. Berry, R. Carey, and A.C. Harris, 2019, Automated core logging technology for geotechnical assessment: A study on core from the Cadia East porphyry deposit: Economic Geology, 114, 1495–1511.

Harris, A.C., D.R. Cooke, J.L. Blackwell, N. Fox, and E.A. Orovan, 2013, Volcano-tectonic setting of world class alkalic porphyry and epithermal Au ± Cu deposits of the southwest Pacific: Society of Economic Geologists Special Publication 17, p. 337–360.

Haschke M, J. Ahmadian M. Murata, and I. McDonald, 2010, Copper mineralization prevented by arc-root delamination during Alpine-Himalayan collision in Central Iran: Economic Geology, 105, 855–865.

Hawkes, D.D., and M.J. Littlefair, 1981, An occurrence of molybdenum, copper, and iron mineralization in the Argentine Islands, West Antarctica: Economic Geology, 76, 898–904.

Holliday, J.R., and D.R. Cooke, 2007, Advances in geological models and exploration methods for copper ± gold porphyry deposits: Decennial International Conference on Mineral Exploration 5, Toronto, Canada, Conference Proceedings, 791–809.

Hollings, P., D.R. Cooke, and A. Clark, 2005, Regional geochemistry of Tertiary volcanic rocks in Central Chile: Implications for tectonic setting and ore deposit genesis: Economic Geology, 100, 887–904.

Hollings, P., R. Wolfe, D.R. Cooke, and P. Waters, 2011, Geochemistry of Tertiary igneous rocks of Northern Luzon, Philippines: Evidence for a back arc-setting for alkali porphyry copper–gold deposits and a case for slab roll-back?: Economic Geology, 106: 1257–1277.

Hoskin, P.W.O., and U. Schaltegger, 2003, The composition of zircon and igneous and metamorphic petrogenesis: Reviews in Mineralogy and Geochemistry, 53, 27−62.

Hou, Z., Z. Yang, X. Qu, X. Meng, Z. Li, G. Beaudoin, Z. Rui, Y. Gao, and K. Zaw, 2009, The Miocene Gangdese porphyry copper belt generated during post-collisional extension in the Tibetan Orogen: Ore Geology Reviews, 36, 25–51.

Hou, Z.Q., H.R. Zhang, X.F. Pan, and Z.M. Yang, 2011, Porphyry Cu(−Mo–Au) systems in non-arc settings, examples from the Tibetan Himalayan orogens and the Yangtze block: Ore Geology Reviews 39, 21-45.

Hu, H., D. Lentz, J.-W. Li, T. McCarron, X.-F. Zhao, and D. Hall, 2015, Re-equilibration processes in magnetite from iron skarn deposits: Economic Geology, 110, 1–8.

Hughes, J.M., and J.F. Rakovan 2015, Structurally robust, chemically diverse: apatite and apatite supergroup minerals: Elements, 11, 165-170

Jackson, L.M., A. Parbhakar-Fox, N. Fox, D.R. Cooke, A.C. Harris, S. Meffre, L. Danyushevsky, K. Goemann, T. Rodemann, G. Gloy, and E. Savinova, 2018, Assessing geo-environmental risk using intact materials for early life-of-mine planning – a review of established techniques and emerging tools, in From Start to Finish: A Life-of-Mine Perspective: The Australasian Institute of Mining and Metallurgy: Carlton, Australia, 1–18.

Kelley, K.D., R.G. Eppinger, J. Lang, S.M. Smith, and D.L. Fey, 2011, Porphyry Cu indicator minerals in till as an exploration tool: Example from the giant Pebble porphyry Cu-Au-Mo deposit, Alaska, USA: Geochemistry: Exploration, Environment, Analysis, 11, 321–334.

Kemp, A.I., C.J. Hawkesworth, G.L. Foster, B.A. Paterson, J.D. Woodhead, , J.M. Hergt, C.M. Gray, M.J. Whitehouse, 2007 Magmatic and crustal differentiation history of granitic rocks from Hf-O isotopes in zircon: Science, 16;315, 980-983.

Kesler, S., and B.H. Wilkinson, 2008; Earth's copper resources estimated from tectonic diffusion of porphyry copper deposits: Geology, 36, 255-258

Kesler, S., L. Jones, and R. Walker, 1975, Intrusive rocks associated with porphyry copper mineralization in island arc magmas: Economic Geology, 70, 515-526.

Lang, J.R., B. Lueck, J.K. Mortensen, J.K. Russell, C.R. Stanley, and J.F.H. Thompson, 1995, Triassic-Jurassic silica-undersaturated and silica saturated alkalic intrusions in the Cordillera of British-Columbia – implications for arc magmatism: Geology, 23, 451–454.

Layton-Matthews, D., C. Hamilton, and M.B. McClenaghan, 2014, Mineral chemistry: modern techniques and applications to exploration: Application of indicator mineral methods to mineral exploration, 26th International Applied Geochemistry Symposium, short course SC07, p. 9-18.

Loader, M.A., 2017, Mineral indicators of porphyry Cu fertility: PhD Thesis, Imperial College London, 436 p.

Loader, M.A., J.J. Wilkinson, and R.N. Armstrong, 2017, The effect of titanite crystallisation on Eu and Ce anomalies in zircon and its implications for the assessment of porphyry Cu deposit fertility: Earth and Planetary Science Letters, 472, 107–119.

Loucks, R., 2012. Chemical characteristics, geodynamic setting and petrogenesis of copper-ore-forming arc magmas: Centre for Exploration Targeting Quarterly Newsletter 19: 1–10.

Loucks, R.R., 2014, Distinctive composition of copper-ore-forming arc magmas: Australian Journal of Earth Sciences, 61: 5-16.

Lowell, J.P., and J.M. Guilbert, 1970, Lateral and vertical alteration-mineralization zoning in porphyry ore deposits: Economic Geology, 65, 373-408.

Mao, M., A.S. Rukhlov, S.M. Rowins, J. Spence, and L.A. Coogan, 2016, Apatite trace element compositions: A robust new tool for mineral exploration: Economic Geology, 111, 1187–1222.

McClenaghan, M.B., 2005, Indicator mineral methods in mineral exploration: Geochemistry: Exploration, Environment, Analysis, 5, 233-245.

Meinert, L.A., G.M. Dipple, and S. Nicolescu, 2005, World skarn deposits: Economic Geology 100th Anniversary Volume, 299–336.

Nadoll, P., J.L. Mauk, R.A. Leveille, and A.E. Koenig, 2015, Geochemistry of magnetite from porphyry Cu and skarn deposits in the southwestern United States: Mineralium Deposita, 50, 493–515.

Pacey, A., J.J. Wilkinson, and D.R. Cooke, in press, Chlorite and epidote mineral chemistry in porphyry ore systems: A case study of the Northparkes district, NSW, Australia: Economic Geology, in press.

Pirajno, F., and T. Zhou, 2015, Intracontinental porphyry and porphyry-skarn mineral systems in Eastern China: Scrutiny of a special case "Made-in-China": Economic Geology, 110, 603-629.

Pisiak, L.K., 2017, Magnetite as an indicator mineral in the exploration of porphyry deposits: A case study in till near the Mount Polley porphyry Cu-Au deposit, British Columbia, Canada: Economic Geology, 112: 919–940.

Richards, J.P., 2009, Postsubduction porphyry Cu-Au and epithermal Au deposits: Products of remelting of subduction-modified lithosphere: Geology, 37, 247–250.

Richards, J.P., 2011a, Magmatic to hydrothermal metal fluxes in convergent and collided margins: Ore Geology Reviews, 40, 1−26.

Richards, J.P., 2011b, High Sr/Y arc magmas and porphyry Cu ± Mo ± Au deposits: Just add water: Economic Geology, 106, 1075–1081.

Richards, J.P., 2015, The oxidation state, and sulfur and Cu contents of arc magmas: implications for metallogeny: Lithos, 233, 27−45.

Rowe, R., 2017, Why and how Uncover?: Science in the Surveys Conference 2017, Conference presentation, Melbourne, Australia, 21 p.

Rowley, P.D., P.L. Williams, D.L. Schmidt, R.L. Reynolds, A.B. Ford, A.H. Clark, E. Farrar, and S.L. McBride, 1975, Copper mineralization along the Lassiter Coast of the Antarctic Peninsula: Economic Geology, 70, 982–987.

Schodde, R., 2017, Recent trends and outlook for global exploration: Conference presentation, Prospectors and Developers Association of Canada Convention, Toronto, 47 p. http://minexconsulting.com/wp-content/uploads/2019/04/Exploration-Trends-and-Outlook-PDAC-Presentation_compressed.pdf

Seedorff, E., J.H. Dilles, J.M. Proffett Jr., M.T. Einaudi, L. Zurcher, W.J.A. Stavast, D.A. Johnson, and M.D. Barton, 2005, Porphyry deposits: Characteristics and origin of hypogene features: Economic Geology 100th Anniversary Volume, 251–298.

Shelton, K., 1983, Composition and origin of ore-forming fluids in a carbonate-hosted porphyry coppe and skarn deposit: A fluid inclusion and stable isotope study of Mines Gaspé, Quebec: Economic Geology, 78, 387–421.

Shen, P., K. Hattori, H. Pan, S. Jackson, and E. Seitmuratova, 2015, Oxidation condition and metal fertility of granitic magmas: Zircon trace-element data from porphyry Cu deposits in the Central Asian orogenic belt: Economic Geology, 110, 1861–1878.

Sievwright, R.H., 2018, Developing magnetite chemistry as an exploration tool for porphyry copper deposits: Ph.D. thesis, Imperial College London, 344 p.

Sillitoe, R.H., 1989, Gold deposits in western Pacific island arcs; the magmatic connection: Economic Geology Monograph 6, 274–291.

Sillitoe, R.H., 1995, Exploration of porphyry copper lithocaps: AUSIMM Publication Series 9: 527−532

Sillitoe, R.H., 1999, Styles of high-sulphidation gold, silver, and copper mineralization in porphyry and epithermal environments: The AusIMM Proceedings, 305, 19–34.

Sillitoe, R.H., 2000, Gold-rich porphyry deposits: Descriptive and genetic models and their role in exploration and discovery: Reviews in Economic Geology, 13, 315−345.

Sillitoe, R.H., 2010, Porphyry-copper systems: Economic Geology, 105, 3-41.

Sillitoe, R.H., 2012, Copper provinces: Society of Economic Geologists Special Publication 16, 1-18.

Stoffregen, R.E., and G.L. Cygan, 1990, An experimental study of Na-K exchange between alunite and aqueous sulfate solutions: American Mineralogist, v. 75, p. 209−220.

Singer, D.A., 1995, World class base and precious metal deposits—A quantitative analysis: Economic Geology, 90, 88–104.

Von Quadt, A., M. Erni, K. Martinek, M. Moll, I. Peytcheva, and C.A. Heinrich, 2011, Zircon crystallization and the lifetimes of ore-forming magmatic-hydrothermal systems: Geology, 39, 731−734.

Watson, E.B., and T.M. Harrison, 2005, Zircon thermometer reveals minimum melting conditions on earliest earth: Science, 308, 841−844.

Webster J.D., and P.M. Piccoli 2015, Magmatic apatite: a powerful, yet deceptive, mineral: Elements, 11, 177-182

Wilkinson J.J., Z. Chang, D.R. Cooke, M. Baker, C.C. Wilkinson, S. Inglis, H. Chen, and J.B. Gemmell, 2015, The chlorite proximitor: A new tool for detecting porphyry ore deposits: Journal of Geochemical Exploration, 152, 10–26.

Wilkinson J.J., M. Baker, D.R. Cooke, C.C. Wilkinson, and S. Inglis, 2017, Exploration targeting in porphyry Cu systems using propylitic mineral chemistry: a case study of the El Teniente deposit, Chile, in Mineral Resources to Discover: Society of Geology Applied to Ore Deposits, 14th Biennial Conference Proceedings, Quebec, v.3, p. 1112-1114.

Wilkinson, J.J., M.J. Baker, D.R. Cooke, and C.C. Wilkinson, in press, Exploration targeting in porphyry Cu systems using propylitic mineral chemistry: a case study of the El Teniente deposit, Chile: Economic Geology, in press.

Wilkinson, B.H., and S.E. Kesler, 2006, Tectonism and exhumation in convergent margin orogens: Insights from ore deposits. Journal of. Geology, 115, 611–627.

Williamson, B.J., R.J. Herrington, and A. Morris, 2016, Porphyry copper enrichment linked to excess aluminium in plagioclase: Nature Geosciences, 9, 237–242.

Wolfe, R., and D.R. Cooke, 2011, Geology of the Didipio region and genesis of the Dinkidi alkalic porphyry Cu–Au deposit and related pegmatites, northern Luzon, Philippines: Economic Geology, 106, 1279–1315.

Yanites, B.J., and S.E. Kesler, 2015, A climate signal in exhumation patterns revealed by porphyry copper deposits: Nature Geoscience, 8, 462–465.

Xiao, B., H. Chen, Y. Wang, J. Han, C. Xu, and J. Yang, 2018, Chlorite and epidote chemistry of the Yandong Cu deposit, NW China: Metallogenic and exploration implications for Paleozoic porphyry Cu systems in the Eastern Tianshan: Ore Geology Reviews, 100, 168–182.

Zellmer, G.F., R.S.J. Sparks, C.J. Hawkesworth, and M. Wiedenbeck, 2003, Magma emplacement and remobilization timescales beneath Montserrat: insights from Sr and Ba zonation in plagioclase phenocrysts. Journal of Petrology, 44, 1413–1431.

Figure 1: Discovery rate versus exploration expenditure: 1950 – 2015. Note that "discoveries" only includes deposits that are "moderate" or larger in size, i.e., > 100 koz Au, > 10 kt Ni, > 100 kt Cu, > 250 kt Zn + Pb, > 5 kt U_3O_8, > 10 Mt Fe, > 20 Mt thermal coal. Please note that world exploration expenditure data was only available since 1975. Source: MinEX Consulting © March 2017 (diagram modified from Schodde, 2017).

Figure 2. Schematic illustration of alteration zoning and overprinting relationships in a porphyry system (modified after Holliday and Cooke 2007; Cooke et al. 2014b, 2017). The multiphase intrusive complex at the center of porphyry deposits typically has potassic alteration developed within and around it. The potassic domain may contain magnetite as a vein and/or alteration mineral, particularly when the intrusive complex has mafic to intermediate compositions. The potassic domain passes outwards laterally to three subfacies of propylitic alteration in volcanic rocks: inner high temperature actinolite subzone; intermediate temperature epidote subzone, and outer low temperature chlorite subzone. Sulfides in the porphyry deposit are typically zoned from a central bornite and/or chalcopyrite-rich domain outwards to a pyrite halo. The dimensions of the pyrite halo vary from deposit to deposit, depending on the amount of sulfur released from the intrusive complex and the oxidized or reduced nature of the country rocks. The pyrite halo typically extends into the epidote subzone of the propylitic zone. At shallow levels, a lithocap may overlie and partially overprint porphyry-style mineralization. The lithocap may host high sulfidation-state mineralization and can cover intermediate sulfidation state epithermal veins. The lithocaps will overprint and be surrounded by propylitic alteration assemblages. The roots of the lithocap lie within the pyrite halo of the porphyry system. The degree of superposition of the lithocap into the porphyry system is contingent on uplift and erosion rates at the time of mineralization, and will vary from province to province, and from district to district. Abbreviations: ab – albite; act – actinolite; anh – anhydrite; Au- gold; bi – biotite; bn – bornite; cb – carbonate; chl – chlorite; cp – chalcopyrite; epi – epidote; gt – garnet; hm – hematite; Kf – K-feldspar; mt – magnetite; py – pyrite; qz – quartz.

Figure 3: CoreScan® image of half of a meter of HQ core from the Cadia East porphyry Au-Cu deposit, Australia. (A) High-resolution true-color photography. (B) Hyperspectral imagery data. In this case, mineralogical products interpreted from hyperspectral data have been draped over the surface topography to observe the relationship between fractures and mineralogy for geotechnical assessment (modified from Harraden et al., 2019).

Figure 4: Zircon as a porphyry indicator mineral. In this schematic example, zircons from the porphyry ore-forming intrusive complex has trace element and isotopic compositions distinct from the barren pre-mineralization intrusion, and also from basement-derived metamict zircons. Because zircons are resistate, they can be detected in stream sediments downstream from the eroded intrusive complex. Analysis of zircon grains from the stream sediment (or till) samples can therefore provide indications of a concealed porphyry deposit upstream of the sample location.

Figure 5: Ce^{4+}/Ce^{3+} for zircon grains from mineralized intrusive complexes versus Cu tonnage (reserves plus past production) of the related porphyry Cu deposits from the Central Asian Orogenic Belt (CAOB). The red boxes represent average ratios of zircon from each rock sample. Diagram modified from Shen et al. (2015).

Figure 6: Magmatic plagioclase compositions from pre-, inter- and late-mineralization porphyry intrusions from La Paloma and Los Sulfatos ore zones, Rio Blanco – Los Bronces – Los Sulfatos district Chile. Also shown for comparative purposes are plagioclase compositions from the barren Monserrat volcano, Caribbean. Diagram modified from Williamson et al. (2016). Data sources: 1 - Williamson et al. (2016), 2 – Zellmer et al. (2003).

Figure 7: Correlation of apatite cathodoluminescence characteristics with the Mn/Fe ratio and abundances of REE in magmatic and hydrothermal apatite from calc-alkaline and alkalic porphyry Cu-Au deposits in British Columbia. Modified from Bouzari et al. (2016).

Figure 8: Discrimination of magmatic (red symbols) and hydrothermal magnetite (blue symbols) based on Ti contents and Ni/Cr values. Modified from Dare et al. (2014).

Figure 9. LA-ICP-MS analyses of epidote and chlorite from the Taldy Bulak porphyry Cu-Au deposit, Kyrgyzstan, highlights coincident anomalies of low As in epidote and high Ti/Sr in chlorite that coincide with the > 600 ppm Cu in soil anomaly. As in epidote data range from 6.69 to 440 ppm. Ti/Sr values for chlorite range from 4.86 to 727. Contours calculated using a minimum curvature grid with open edges. Samples lacking epidote and/or chlorite analyses were treated as nulls. Mean values were calculated using between 1 and 10 valid epidote or chlorite analyses per sample location. Geological map and Cu assay data from Orsu Metals Corporation – Updated Technical Report on the Taldy Bulak Property, Kyrgyzstan, March 22, 2010.

Figure 10. Mankayan lithocap, Philippines. The location of the Lepanto enargite deposit and Far Southeast porphyry Cu-Au deposit is shown in grey fill and vertical striped fill, respectively, with surface outcrops of the lithocap marked by dashed lines. A) Alunite SWIR results (average of three measurements per sample). (B) 1000000 * Pb / (Na+K) ratios for whole rock samples. (C) 100 * La/Pb ratios for whole rock samples. For panels (B) and (C), statistical bins were determined based on natural breaks in the whole rock geochemical data. All whole rock data screened – only alunite-bearing samples with less than 0.1 % Cu and 0.1 g/t Au plotted. Diagram modified from Chang et al. (2011).

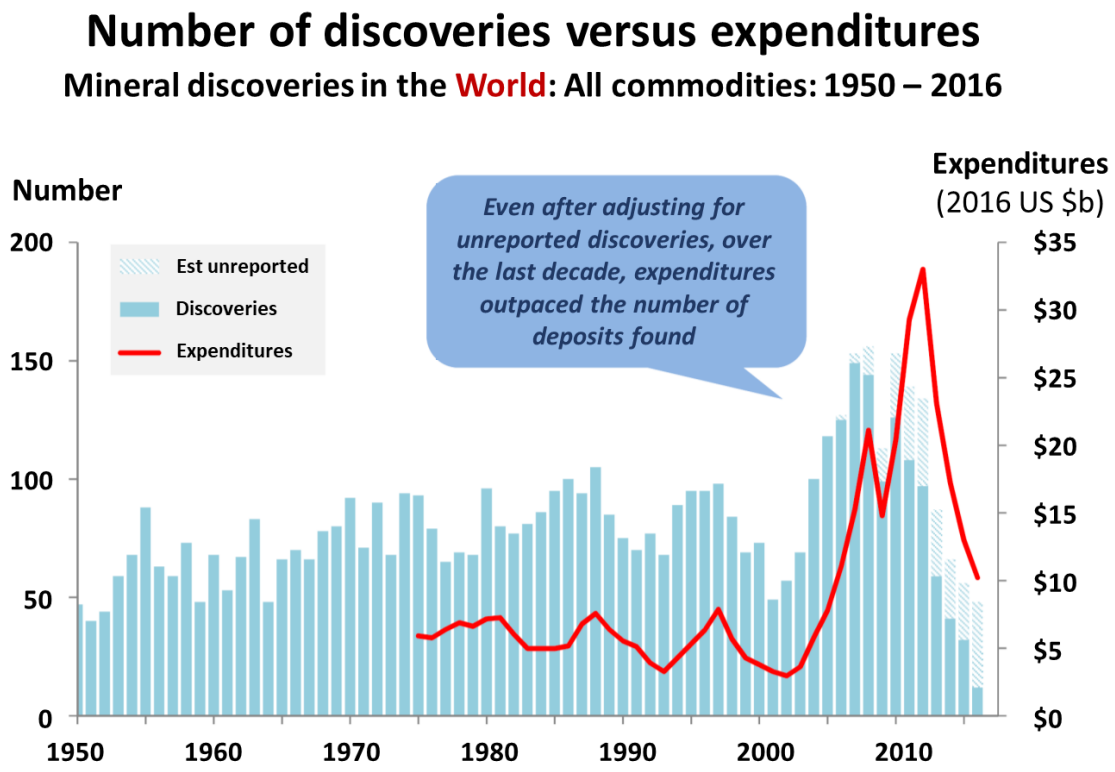

Figure 1: Discovery rate versus exploration expenditure: 1950 – 2015. Note that "discoveries" only includes deposits that are "moderate" or larger in size, i.e., > 100 koz Au, > 10 kt Ni, > 100 kt Cu, > 250 kt Zn + Pb, > 5 kt U_3O_8, > 10 Mt Fe, > 20 Mt thermal coal. Please note that world exploration expenditure data was only available since 1975. Source: MinEX Consulting © March 2017 (diagram modified from Schodde, 2017).

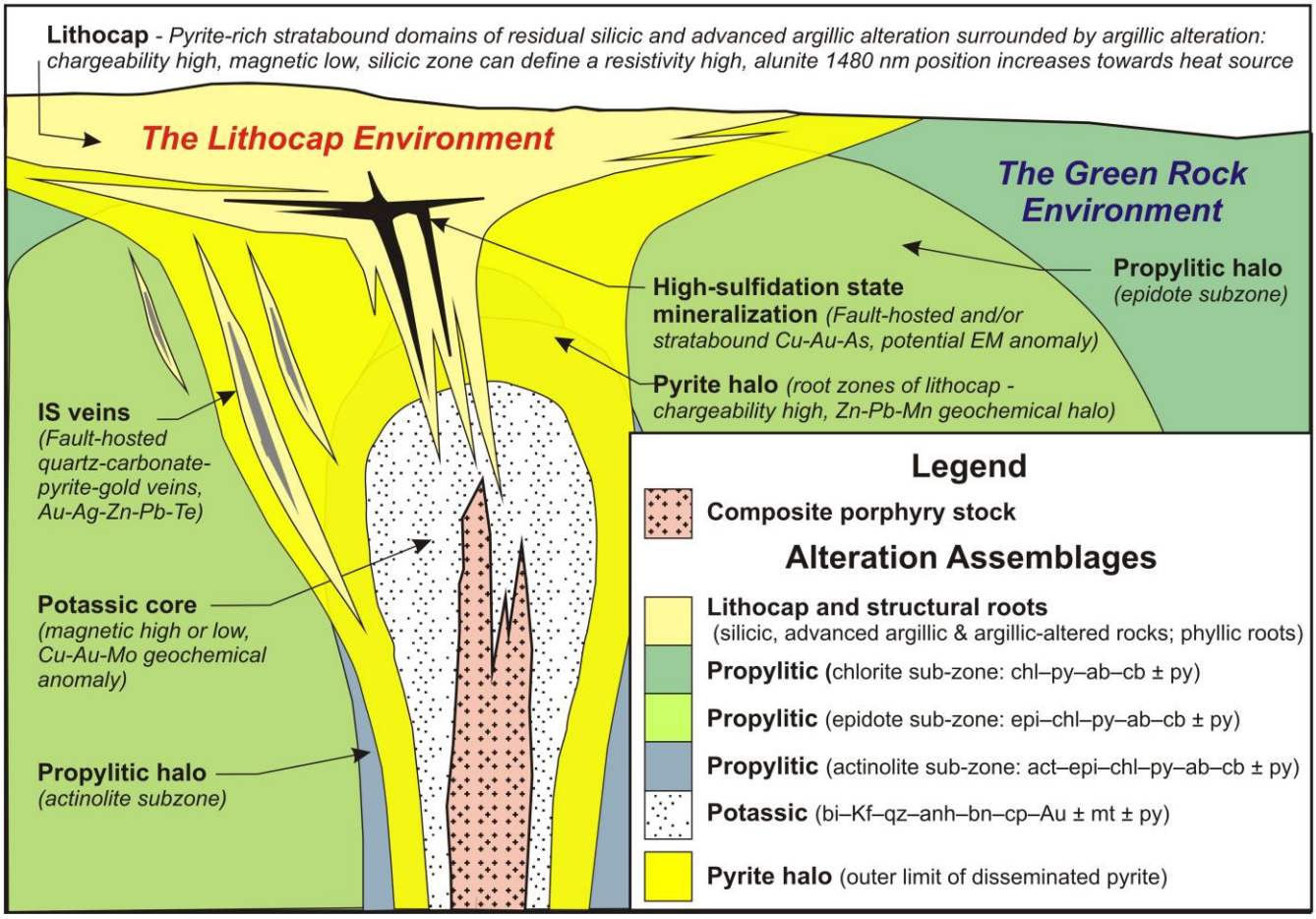

Figure 2. Schematic illustration of alteration zoning and overprinting relationships in a porphyry system (modified after Holliday and Cooke 2007; Cooke et al. 2014b, 2017). The multiphase intrusive complex at the center of porphyry deposits typically has potassic alteration developed within and around it. The potassic domain may contain magnetite as a vein and/or alteration mineral, particularly when the intrusive complex has mafic to intermediate compositions. The potassic domain passes outwards laterally to three subfacies of propylitic alteration in volcanic rocks: inner high temperature actinolite subzone; intermediate temperature epidote subzone, and outer low temperature chlorite subzone. Sulfides in the porphyry deposit are typically zoned from a central bornite and/or chalcopyrite-rich domain outwards to a pyrite halo. The dimensions of the pyrite halo vary from deposit to deposit, depending on the amount of sulfur released from the intrusive complex and the oxidized or reduced nature of the country rocks. The pyrite halo typically extends into the epidote subzone of the propylitic zone. At shallow levels, a lithocap may overlie and partially overprint porphyry-style mineralization. The lithocap may host high sulfidation-state mineralization and can cover intermediate sulfidation state epithermal veins. The lithocaps will overprint and be surrounded by propylitic alteration assemblages. The roots of the lithocap lie within the pyrite halo of the porphyry system. The degree of superposition of the lithocap into the porphyry system is contingent on uplift and erosion rates at the time of mineralization, and will vary from province to province, and from district to district. Abbreviations: ab – albite; act – actinolite; anh – anhydrite; Au- gold; bi – biotite; bn – bornite; cb – carbonate; chl – chlorite; cp – chalcopyrite; epi – epidote; gt – garnet; hm – hematite; Kf – K-feldspar; mt – magnetite; py – pyrite; qz – quartz

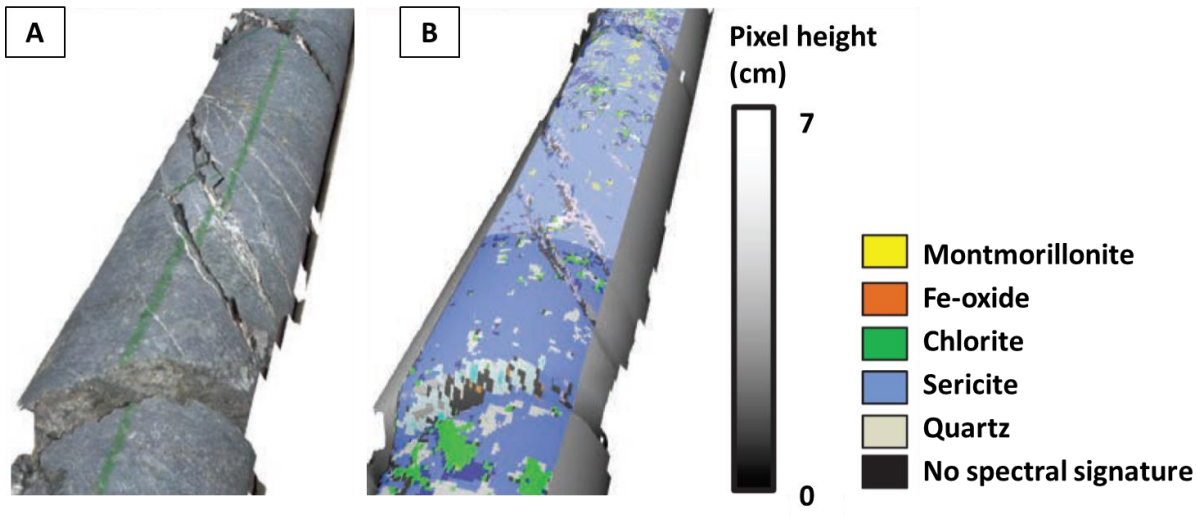

Figure 3: CoreScan® image of half of a meter of HQ core from the Cadia East porphyry Au-Cu deposit, Australia. (A) High-resolution true-color photography. (B) Hyperspectral imagery data. In this case, mineralogical products interpreted from hyperspectral data have been draped over the surface topography to observe the relationship between fractures and mineralogy for geotechnical assessment (modified from Harraden et al., 2019).

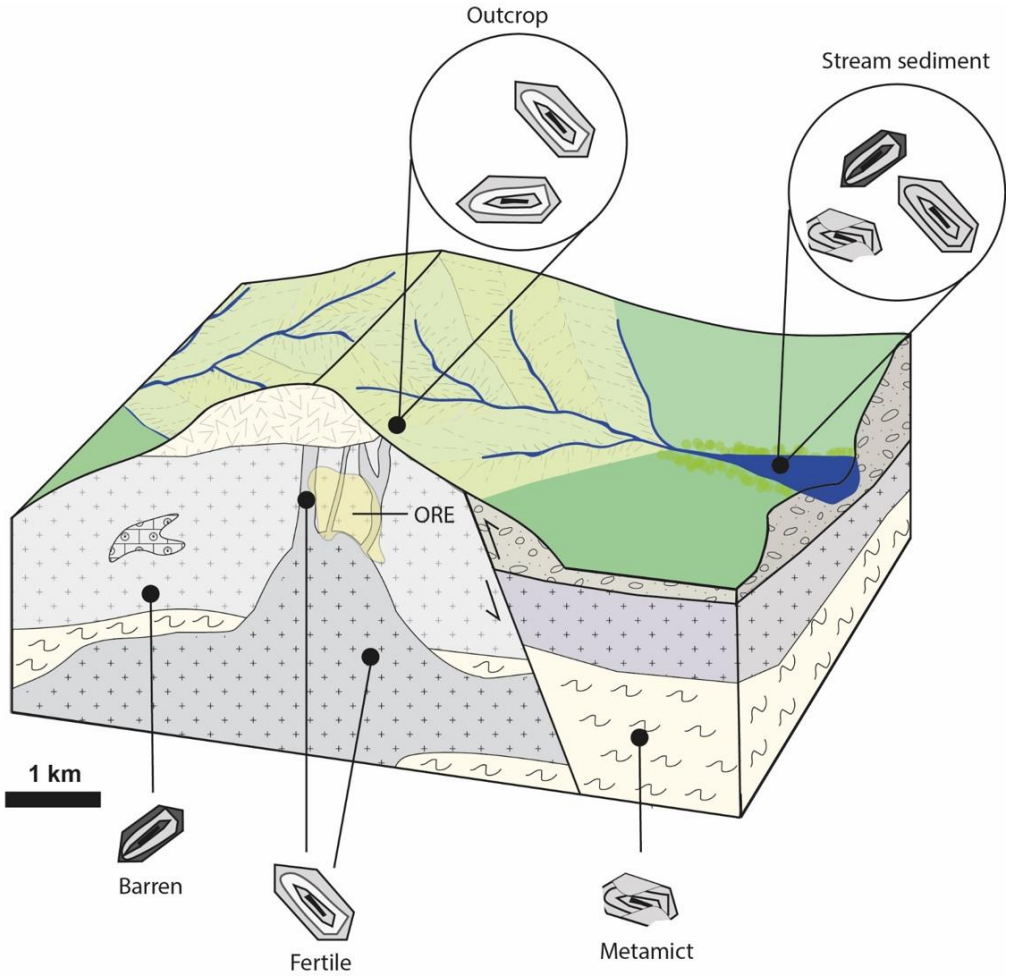

Figure 4: Zircon as a porphyry indicator mineral. In this schematic example, zircons from the porphyry ore-forming intrusive complex has trace element and isotopic compositions distinct from the barren pre-mineralization intrusion, and also from basement-derived metamict zircons. Because zircons are resistate, they can be detected in stream sediments downstream from the eroded intrusive complex. Analysis of zircon grains from the stream sediment (or till) samples can therefore provide indications of a concealed porphyry deposit upstream of the sample location.

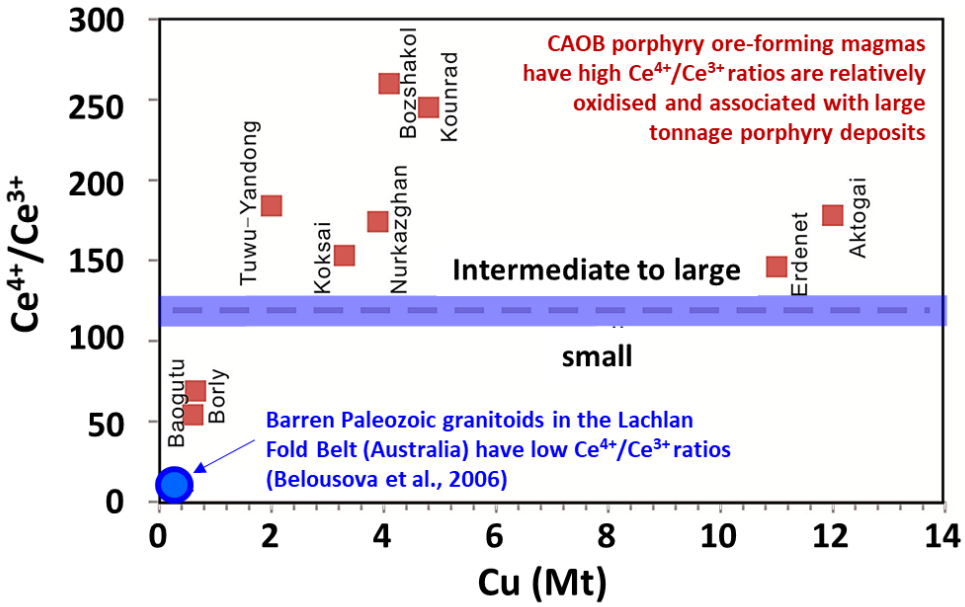

Figure 5: Ce^{4+}/Ce^{3+} ratios for zircon grains from mineralized intrusive complexes versus Cu tonnage (reserves plus past production) of the related porphyry Cu deposits from the Central Asian Orogenic Belt (CAOB). The red boxes represent average ratios of zircon from each rock sample. Diagram modified from Shen et al. (2015).

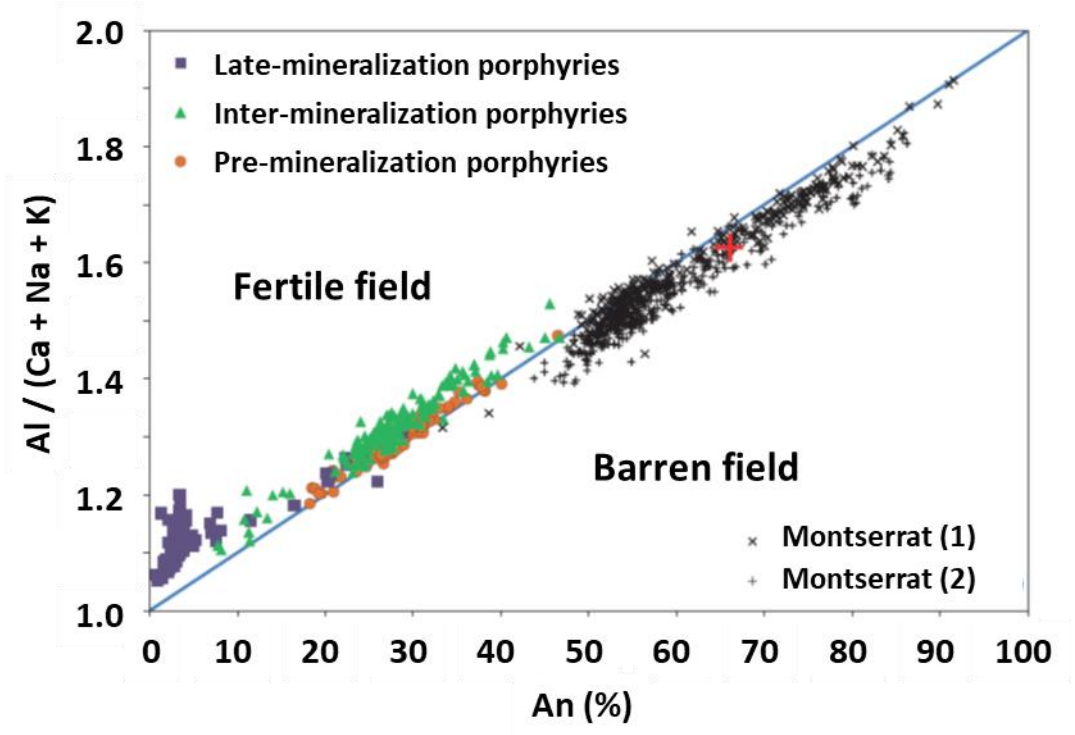

Figure 6: Magmatic plagioclase compositions from pre-, inter- and late-mineralization porphyry intrusions from La Paloma and Los Sulfatos ore zones, Rio Blanco – Los Bronces – Los Sulfatos district Chile. Also shown for comparative purposes are plagioclase compositions from the barren Monserrat volcano, Caribbean. Diagram modified from Williamson et al. (2016). Data sources: 1 - Williamson et al. (2016), 2 – Zelmer et al. (2003).

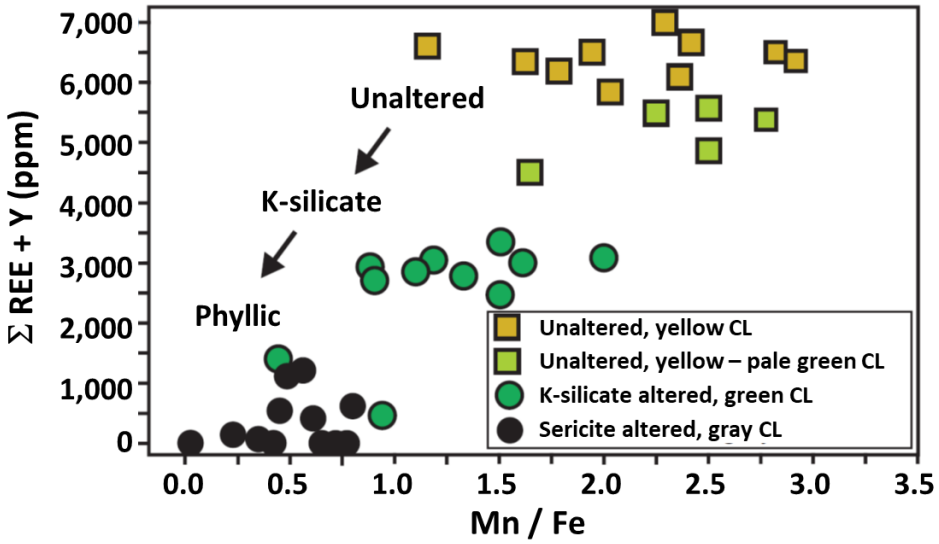

Figure 7: Correlation of apatite luminescence characteristics with the Mn/Fe ratio and abundances of REE in magmatic and hydrothermal apatites from calc-alkaline and alkalic porphyry Cu-Au deposits in British Columbia. Modified from Bouzari et al. (2016).

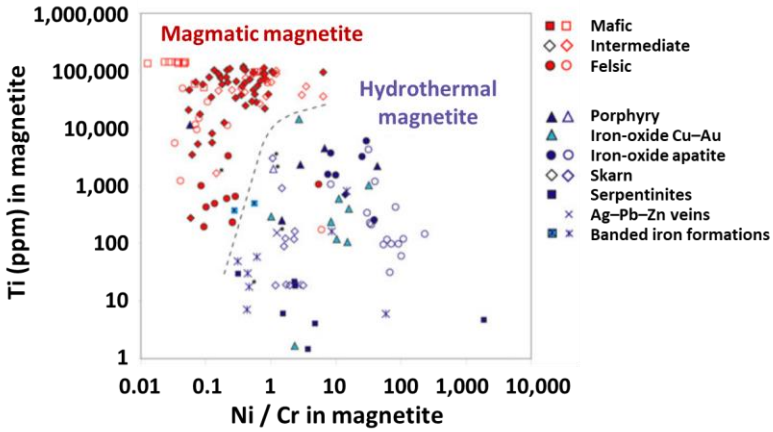

Figure 8: Discrimination of magmatic (red symbols) and hydrothermal magnetite (blue symbols) based on Ti contents and Ni/Cr ratios. Modified from Dare et al. (2014).

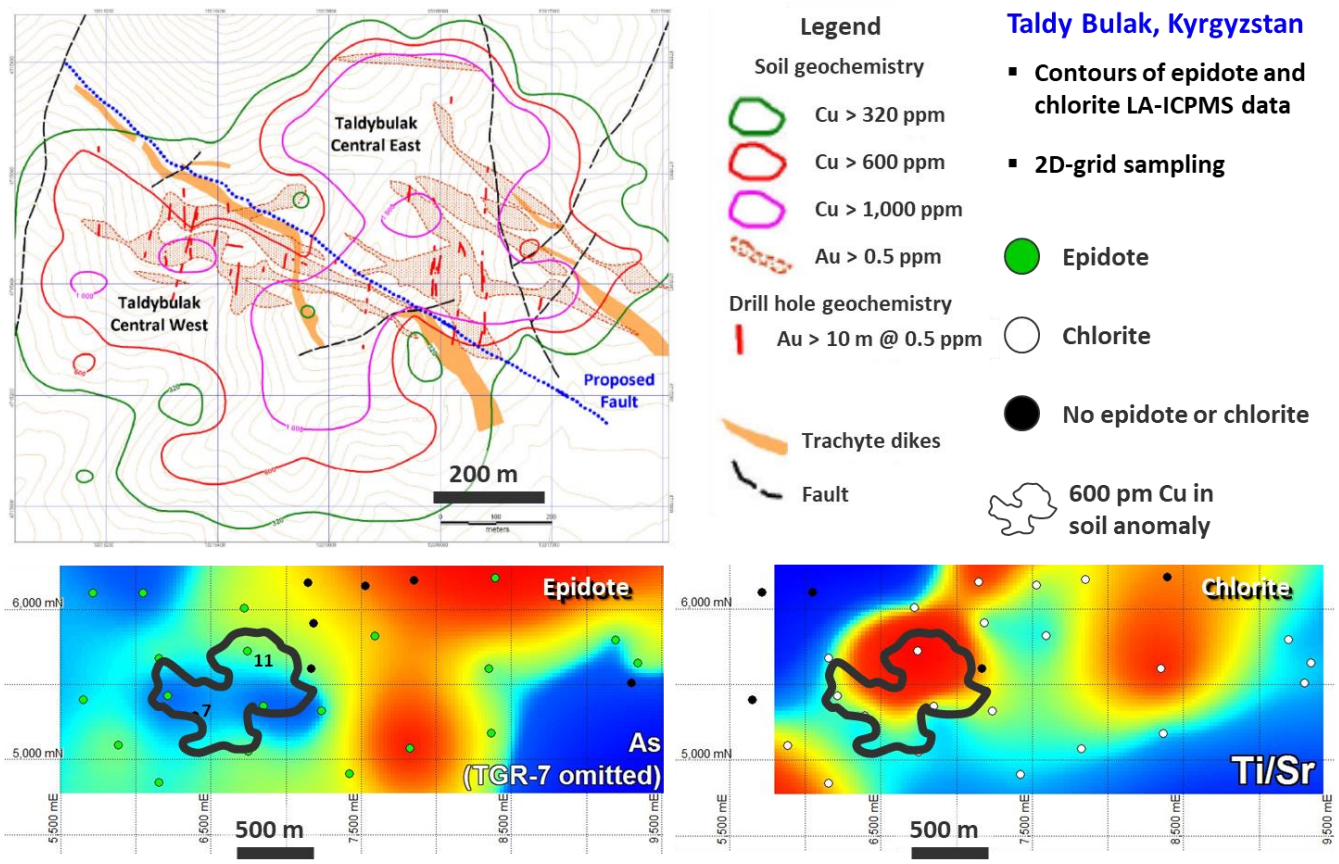

Figure 9. LA-ICP-MS analyses of epidote and chlorite from the Taldy Bulak porphyry Cu-Au deposit, Kyrgyzstan, highlights coincident anomalies of low As in epidote and high Ti/Sr ratios in chlorite that coincide with the > 600 ppm Cu in soil anomaly. As in epidote data range from 6.69 to 440 ppm. Ti/Sr ratios for chlorite range from 4.86 to 727. Geological map and Cu assay data from Orsu Metals Corporation – Updated Technical Report on the Taldy Bulak Property, Kyrgyzstan, March 22, 2010.

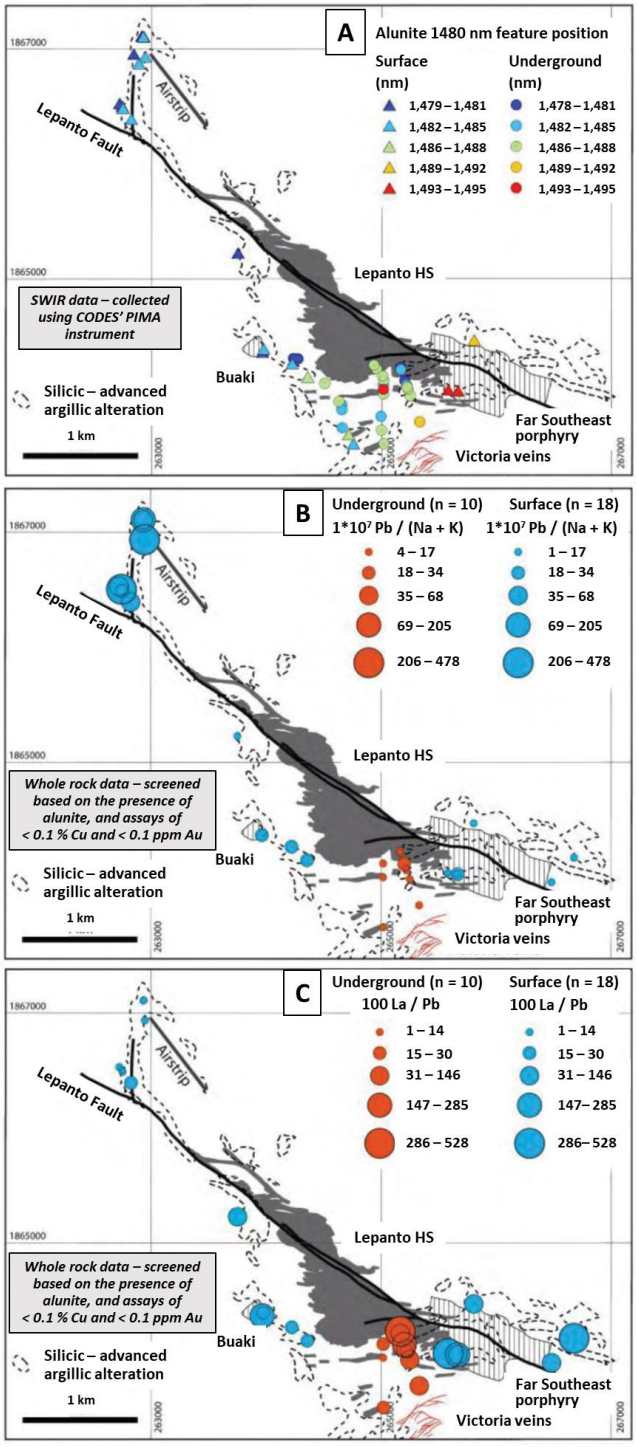

Figure 10. Mankayan lithocap, Philippines. The location of the Lepanto enargite deposit and Far Southeast porphyry Cu-Au deposit is shown in grey fill and vertical striped fill, respectively, with surface outcrops of the lithocap marked by dashed lines. (A) Alunite SWIR results. (B) 1000000 * Pb / (Na+K) ratios for whole rock samples. (C) 100 * La/Pb ratios for whole rock samples. All whole rock data screened – only alunite-bearing samples with less than 0.1 % Cu and 0.1 g/t Au plotted. Diagram modified from Chang et al. (2011).